ATHENS UNIVERSITY OF ECONOMICS AND BUSINESS

DEPARTMENT OF STATISTICS

POSTGRADUATE PROGRAM

ON THE PROBABILITY DISTRIBUTION OF THE DURATION OF DRY AND WET SPELLS IN PROCESSES OF SPATIALLY AVERAGED RAIN RATE

By

Ioannis A. Gritsis

A THESIS

Submitted to the Department of Statistics
of the Athens University of Economics and Business
in partial fulfillment of the requirements for
the degree of Master of Science in Statistics

Athens, Greece
1997

ISBN : 960-7929-04-7

ATHENS UNIVERSITY OF ECONOMICS AND BUSINESS

DEPARTMENT OF STATISTICS

ON THE PROBABILITY DISTRIBUTION OF THE DURATION OF DRY AND WET SPELLS IN PROCESSES OF SPATIALLY AVERAGES RAIN RATE

By

Ioannis Gritsis

A THESIS

Submitted to the Department of Statistics
of the Athens University of Economics and Business
in partial fulfillment of the requirements for
the degree of Master of Science in Statistics

Athens, Greece
1997

ΟΙΚΟΝΟΜΙΚΟ ΠΑΝΕΠΙΣΤΗΜΙΟ
ΑΘΗΝΩΝ

ΤΜΗΜΑ ΣΤΑΤΙΣΤΙΚΗΣ

ΠΕΡΙ ΤΗΣ ΚΑΤΑΝΟΜΗΣ ΠΙΘΑΝΟΤΗΤΑΣ ΤΗΣ ΔΙΑΡΚΕΙΑΣ ΞΗΡΩΝ ΚΑΙ ΥΓΡΩΝ ΠΕΡΙΟΔΩΝ ΣΕ ΑΝΕΛΙΞΕΙΣ ΧΩΡΙΚΩΝ ΜΕΣΩΝ ΕΝΤΑΣΕΩΣ ΒΡΟΧΗΣ

Ιωάννης Γκρίτσης

ΔΙΑΤΡΙΒΗ

Που υποβλήθηκε στο Τμήμα Στατιστικής
του Οικονομικού Πανεπιστημίου Αθηνών
ως μέρος των απαιτήσεων για την απόκτηση
Μεταπτυχιακού Διπλώματος Ειδίκευσης στη Στατιστική

Αθήνα
1997

ATHENS UNIVERSITY OF ECONOMICS AND BUSINESS

DEPARTMENT OF STATISTICS

A Thesis submitted in partial fulfillment of
the requirements for the degree of
Master of Science

ON THE PROBABILITY DISTRIBUTION OF THE DURATION OF DRY AND WET SPELLS IN PROCESSES OF SPATIALLY AVERAGED RAIN RATE

Ioannis Gritsis

Supervisor :
Dr. Ch. Pavlopoulos

External examiner :
Professor Benjamin Kedem
Departmentof Mathematics
University of Maryland,
USA

Approved by the Graduate Committee

Professor E. Xekalaki
Director of the Graduate Program
September 1997

DEDICATION

To my parents

ACKNOWLEDGEMENTS

I would like to express my sincere thanks to my supervisor Dr. Harry Pavlopoulos for suggesting the problem, his helpful comments and assistance throughout the period of this dissertation. Thanks are also expressed to Dr. David Short of NASA/Goddard Space Flight Center for making available to us the TOGA-COARE data set. I also thank Mr. Stefanos Giakoumatos for his help with some programming and software applications.

VITA

Born in Athens, in May 1973. In 1995, he earned his B.Sc. degree in *Theoretical and Applied Statistics* from the Department of Statistics of the Athens University of Economics and Business.

Ioannis Gritsis

ON THE PROBABILITY DISTRIBUTION OF THE DURATION OF DRY AND WET SPELLS IN PROCESSES OF SPATIALLY AVERAGED RAIN RATE

1997

ABSTRACT

The lognormal, inverse gaussian, and gamma probability distribution models are fitted to data of durations of dry and wet epochs obtained from real time series of spatially averaged rain rate. Each model's parameters are estimated by the statistical methods of moments and maximum likelihood, based on TOGA-COARE measurements of tropical rainfall. The hypotheses of independence and identical distribution (i.i.d.) among durations of dry or wet epochs are tested. The effects of variation of the spatial scale on the values of moments of dry and wet epoch durations are also investigated, pointing to self-similarity of the underlying probability distributions, or at least simple scaling of their moments.

Ιωάννης Γκρίτσης

ΠΕΡΙ ΤΗΣ ΚΑΤΑΝΟΜΗΣ ΠΙΘΑΝΟΤΗΤΑΣ ΤΗΣ ΔΙΑΡΚΕΙΑΣ ΞΗΡΩΝ ΚΑΙ ΥΓΡΩΝ ΠΕΡΙΟΔΩΝ ΣΕ ΑΝΕΛΙΞΕΙΣ ΧΩΡΙΚΩΝ ΜΕΣΩΝ ΕΝΤΑΣΕΩΣ ΒΡΟΧΗΣ

1997

ΠΕΡΙΛΗΨΗ

Οι κατανομές πιθανότητας λογαριθμική κανονική, αντίστροφη Gauss, και γάμμα, ελέγχονται ως προς την προσαρμογή τους στις διάρκειες ξηρών και υγρών περιόδων οι οποίες προκύπτουν από πραγματικές χρονοσειρές χωρικών μέσων εντάσεως βροχής. Οι παράμετροι καθενός από τα τρία υποδείγματα εκτιμώνται με τις στατιστικές μεθόδους των ροπών και μέγιστης πιθανοφάνειας, με βάση μετρήσεις τροπικών βροχοπτώσεων από το πείραμα TOGA-COARE. Επίσης, γίνεται έλεγχος των υποθέσεων ανεξαρτησίας και ταυτοτικής κατανομής μεταξύ των διαρκειών ξηρών ή υγρών περιόδων. Τέλος, μελετάται η επίδραση της μεταβολής της χωρικής κλίμακας στις τιμές των ροπών ξηρών και υγρών περιόδων, αναδεικνύοντας την αυτο-ομοιότητα της αντίστοιχης υποκείμενης κατανομής πιθανότητας, ή τουλάχιστον απλή κλιμάκωση των αντίστοιχων ροπών.

TABLE OF CONTENTS

1 INTRODUCTION **1**

2 LITERATURE SURVEY AND OBJECTIVES **3**

2.1 EMPIRICAL LOGNORMALITY OF CLOUD CHARACTERISTICS 3

2.2 INVERSE GAUSSIANITY EMERGING FROM STOCHASTIC BUDGET OF MOISTURE 6

2.3 THE CANDIDACY OF GAMMA DISTRIBUTION 10

3 DATA AND TESTING FOR RANDOMNESS **13**

3.1 DESCRIPTION OF THE DATA 13

3.2 TESTING RANDOMNESS 15

3.2.1 DRY SPELLS 16

3.2.2 WET SPELLS 17

4 ESTIMATION AND GOODNESS OF FIT **18**

4.1 ESTIMATION OF PARAMETERS 18

4.2 TESTS AND COMPARISON OF GOODNESS OF FIT 21

4.2.1 DRY EPOCH DURATION 24

4.2.2 WET EPOCH DURATION 27

5 SCALING EFFECTS **31**

5.1 SCALING OF DRY SPELLS 35

5.2 SCALING OF WET SPELLS 41

6 CONCLUSION **49**

REFERENCES **54**

APPENDIX

LIST OF TABLES

Table 1. Numbers of dry and wet blocks of the time series which correspond to the five area sizes. 14

Table 2. Results obtained after the application of the Runs test to the dry sequences. 16

Table 3. Results obtained after the application of the Runs test to the wet sequences. 17

Table 4. Lognormal, Inverse Gaussian and Gamma parameters of Dry phases for each time series..... 20

Table 5. Lognormal, Inverse Gaussian and Gamma parameters of Wet phases for each time series..... 21

Table 6. Goodness of fit of the three probability models for dry durations corresponding to 2×2 km^2 area..... 24

Table 7. Goodness of fit of the three probability models for dry durations corresponding to 4×4 km^2 area..... 24

Table 8. Goodness of fit of the three probability models for dry durations corresponding to 6×6 km^2 area..... 25

Table 9. Goodness of fit of the three probability models for dry durations corresponding to 8×8 km^2 area..... 25

Table 10. Goodness of fit of the three probability models for dry durations corresponding to 10×10 km^2 area..... 26

Table 11. Goodness of fit of the three probability models for wet durations corresponding to 2×2 km^2 area.....27

Table 12. Goodness of fit of the three probability models for wet durations corresponding to 4×4 km^2 area.....28

Table 13. Goodness of fit of the three probability models for wet durations corresponding to 6×6 km^2 area.....28

Table 14. Goodness of fit of the three probability models for wet durations corresponding to 8×8 km^2 area.....29

Table 15. Goodness of fit of the three probability models for wet durations corresponding to 10×10 km^2 area.....29

Table 16. Lognormal and Inverse Gaussian mean and variance of dry durations. 32

Table 17. Lognormal and Inverse Gaussian mean and variance of wet durations.....32

Table 18. The logarithms of the ratios of the means of Dry epoch durations, for scale λ, under the Lognormal and Inverse Gaussian models (MLE and MME), the scale λ and its logarithm.....36

Table 19. Squared correlation, Slope, and Sum of Squared Residuals of regressions of $\log(M_\lambda/M_1)$ on $\log\lambda$ under LN and IG models for dry durations. 36

Table 20. The logarithms of the ratios of the variances of Dry epoch durations, for scale λ, under the Lognormal and Inverse Gaussian models (MLE and MME), the scale λ and its logarithm.....38

Table 21. Squared correlation, Slope, and Sum of Squared Residuals of regressions of $\log(V_\lambda/V_1)$ on $\log\lambda$ under LN and IG models for dry durations. 38

Table 22. Tabulation of Dry sample moments of order k=1,..., 20 and the results (slope, R squared, and Sum of Squared Residuals) of regressions of $\log[\hat{M}_\lambda(k)/\hat{M}_1(k)]$ on $\log\lambda$.....40

Table 23. Tabulation of the logarithms of the ratios of the means of Wet epoch durations, for scale λ, under the Lognormal and Inverse Gaussian models (MLE and MME), the scale λ and its logarithm. 41

Table 24. Squared correlation, Slope, and Sum of Squared Residuals of regressions of $\log(M_\lambda/M_1)$ on $\log\lambda$ under LN and IG models for wet durations. 42

Table 25. Tabulation of the logarithms of the ratios of the variances of Wet epoch durations, for scale λ, under the Lognormal and Inverse Gaussian models (MLE and MME), the scale λ and its logarithm. 43

Table 26. Squared correlation, Slope, and Sum of Squared Residuals of regressions of $\log(V_\lambda/V_1)$ on $\log\lambda$ under LN and IG models for wet durations.....43

Table 27. Tabulation of Wet sample moments of order k=1,...,20 and the results (slope, R squared, and Sum of Squared Residuals) of regressions of $\log[\hat{M}_\lambda(k)/\hat{M}_1(k)]$ on $\log\lambda$.....46

LIST OF FIGURES

Figure 1. Regressions of $\log(M_\lambda/M_1)$ on $\log\lambda$ under LN and IG model for dry durations. 37

Figure 2. Regressions of $\log(V_\lambda/V_1)$ on $\log\lambda$ under LN and IG model for dry durations. 39

Figure 3. Regressions of $\log(M_\lambda/M_1)$ on $\log\lambda$ under LN and IG model for wet durations. 42

Figure 4. Regressions of $\log(V_\lambda/V_1)$ on $\log\lambda$ under LN and IG model for wet durations. 44

Figure 5. Regressions of $\log[\hat{M}_\lambda(k)/\hat{M}_1(k)]$ on $\log\lambda$ for order k=1, 2, 10, 20 of wet sample moments. 47

Figure 6. Plot of the slope A(k) versus the order k=1,..., 20 of wet sample moments. 48

CHAPTER 1

INTRODUCTION

Rainfall is undoubtedly a physical process of extremely high variability, in both space and time, difficult to measure, model, and predict, despite a growing scientific interest in understanding its properties and complex structure, either in the time domain, or in the space domain, or in both. Given a fixed geographic region S, and an instantaneous map (or snapshot) of rain intensities (measured in mm/hr) over S at a fixed instant of time, one may consider such a map as being a realization of a random field. Then, one may obtain the spatial average of these intensities over any sub-region A of S (i.e. $A \subseteq S$), and this average may be considered as being the value of a single random variable. Letting the time flow, and obtaining the spatial average of rain intensity over the same sub-region A, for each single instant of time, a random function of time will emerge, which may be considered as being a sample function from a stochastic process referred to as **spatially averaged rain rate process** over A. Since rainfall is an intermittent phenomenon, stopping and restarting off and on in an alternating manner, every sample function of any spatially averaged rain rate process over any region, is bound to be a non-negative function, presumably continuous, at least when the region over which the spatial averages are obtained is large enough, attaining positive values when it rains somewhere in the region, and zero value when it does not rain anywhere in the region. The disjoint time intervals supporting the positive values are referred to as **wet epochs** (or wet spells), and the also disjoint time intervals where the zero value is attained are referred to as **dry epochs** (or dry spells). The subject of interest in this dissertation is the probability

distribution of the duration of wet and of dry epochs of spatially averaged rain rate processes, and the presentation of the material is organized as follows.

Section 2 is a review of some literature on the basis of which the lognormal, inverse Gaussian, and gamma probability distributions are selected as candidate parametric models for the probability distribution of wet and dry epoch duration.

Section 3 is concerned with testing the hypotheses of independent and identically distributed (i.i.d.) values for the data of dry and wet epoch durations. These data have been obtained from the analysis of real measurements of rain rate, collected during the 1992-93 TOGA-COARE experiment in a tropical region, and they are described in detail. To test these hypotheses is of interest here, because their truth is implied in the recent work of Freidlin and Pavlopoulos (1997), which is also the work suggesting the inverse Gaussian as being an appropriate model for the probability distribution of dry and wet epoch durations. These tests have been made on the basis of *runs above and below the median*, using the Wald-Wolfowitz statistic.

Section 4 is concerned with the parameter estimation and the goodness of fit of each one of the above three parametric models to data of dry and wet epoch durations, based on the χ^2-test statistic.

Section 5 is a first attempt to identify any scaling properties of the probability distributions of dry and wet epoch durations, with respect to magnification of the spatial scale $0 < \lambda \leq 1$ of the region over which rain rate is averaged. Section 6 concludes this dissertation with a summary of the obtained results, and some complementary comments.

CHAPTER 2

LITERATURE SURVEY AND OBJECTIVES

2.1 Empirical Lognormality of Cloud Characteristics

The occurrence of rainfall events in space and time is intimately linked with the physical processes of formation, growth, and dissipation of clouds. Key variables used in order to quantify measurable characteristics of a cloud, whether in motion or stationary, are discerned into two main categories, one of the so called extensive or geometric cloud variables, and the other of the intensive cloud variables. The class of extensive cloud variables contains variables which quantify the size or the geometry of the cloud, such as horizontal dimension (or diameter), vertical dimension (or height), area of vertical projection, and volume of the cloud. On the other hand, the class of intensive cloud variables contains variables which quantify the strength or the potential of the cloud with respect to the amount of water content held in it. Such variables are the lifetime (or duration) of a cloud, the volume or the mass of rainfall produced by it, and its intensity which is defined as the ratio of the produced rainfall volume over the lifetime of the cloud. The works of Biondini (1976), Lopez (1977), and Houze and Cheng (1977) unanimously reveal that the empirical probability distribution for many of the extensive and intensive variables of clouds, seem to conform quite well to the lognormal model. This empiricism is confirmed in several cloud populations from different geographic regions and during different seasons. In particular, Biondini (1976) reported that during the 1968-70 EML experiment near Miami, Florida, the logarithms of rainfall volumes, and the logarithms of lifetimes of clouds that produced rainfall, followed a normal probability distribution, regardless

of their classification to dissipating stationary clouds and to merging clouds in motion. Lognormality was also significantly evident in the empirical probability distribution of the corresponding intensities of the studied cloud population.

Lopez (1977) reported significant evidence for lognormality of height, horizontal dimension, and also of duration of clouds, based on radar echo measurements on different cloud populations from Venezuela (1973), Puerto Rico (1955), Arizona (1958, 1967), Massachusetts (1949), N.W. Atlantic (1976), and elsewhere. Moreover, Houze and Cheng (1977) presented a detailed analysis of cloud populations observed by radar echoes during the three phases of the well known GATE experiment, conducted in the summer of 1974 in the Eastern tropical Atlantic, off the West coast of Africa. The results reported in that study, confirmed that in all three phases of GATE, the echo heights, the echo durations, and also the echo areas covered by clouds followed lognormal probability distributions.

In an effort to provide an explanation of this omnipresent empirical lognormality in cloud characteristics, Biondini (1976) and Lopez (1977) have resorted to the *Law of Proportionate Effect (LPE)*, which is the main mathematical scheme associated with the genesis of lognormal distributions; see Aitchison and Brown (1963), Crow and Shimizu (1988).

From Crow and Shimizu (1988), and from Kedem and Chiu (1987b), it is clear that the lognormal distribution may not be the best model for rain rate. However, Kedem and Chiu (1987b), argue that the fit of lognormal to area averaged rain rate improves as the area size increases. This very conclusion has also been reached by Pavlopoulos and Kedem (1992), though in a different way.

Biondini's approach is reducing the problem to the explanation of lognormality in the extensive cloud variables only, under the somewhat ad-hoc

assumption that there is a power law relationship between extensive and intensive cloud variables. That is, if E denotes any one of the extensive variables, and if I is any one of the intensive variables, Biondini assumes that there is a relationship of the form $I = a \cdot E^b$ (or equivalently $\log I = \log a + b \cdot \log E$) between them. Under such a relationship, of course, if E is lognormally distributed, then I will have to be lognormally distributed as well, however with different parameter values. Consequently, formulating a stochastic differential equation analogue of the law of proportionate effect, as a continuous time model driven by Brownian motion for the growth of cloud size, Biondini argues heuristically that the probability distribution of cloud size is indeed lognormal.

The approach taken by Lopez is somewhat different, although he also tried to introduce the law of proportionate effect in terms of a growth process for cloud parcels. The assumptions made by Lopez were two. According to the first assumption, a cloud parcel grows due to the entrainment of moist air from the surrounding environment into the cloud, so that the rate of entrainment increases proportionally with the size of the cloud parcel. According to the second assumption, the size of a cloud grows due to a merging process of smaller cloud elements, where the rate of merging is again randomly proportional to the size of the merging elements.

In light of the above comments, it becomes rather interesting to investigate the plausibility of lognormality in the probability distribution of *rainfall duration* itself, instead of *cloud duration*. Indeed, during the lifetime of a cloud, if any rain is produced by it, this rain may fall during one single sub-interval, or it may fall intermittently during several sub-intervals of the cloud's lifetime. However, the current interest here is not on the duration of rainfall produced by single clouds, but

on duration of spatially averaged rainfall produced by whole systems of clouds over the region of interest.

2.2 Inverse Gaussianity Emerging from Stochastic Budget of Moisture

In a more recent work by Freidlin and Pavlopoulos (1997, hereafter abbreviated FP), a new stochastic model has been proposed in order to describe the temporal variability of the amount of moisture contained in the atmospheric column above a fixed region. A most interesting feature of the model is that it accounts for the intermittent behavior of rainfall produced in the column, in terms of *a hysteresis effect* of the moisture content process between two fixed threshold values $0<x_0<x_1<\infty$. For a coherent presentation of the FP model some notation is introduced. Without loss of generality, suppose that the column is not precipitating at an initial instant $t=\xi_0$. Eventually, the column will start precipitating at some random instant $\tau_1>\xi_0$, it will stop again at a sequel random instant $\xi_1>\tau_1>\xi_0$, it will restart precipitating at a later random instant $\tau_2>\xi_1>\tau_1>\xi_0$, then it will stop anew at a sequel random instant $\xi_2>\tau_2>\xi_1>\tau_1>\xi_0$, and so on ad infinitum. For each $n\geq 1$, the so defined random time intervals $\Phi_n=[\xi_{n-1},\tau_n)$ are the *dry epochs* of the column, the random intervals $\Psi_n=[\tau_n,\xi_n)$ are the *wet epochs* of the column, and $\phi_n=\tau_n-\xi_{n-1}$ and $\psi_n=\xi_n-\tau_n$ are the corresponding dry and wet epoch durations. The set $T_1=\bigcup_{n\geq 1}\Phi_n$ is the set of all dry instants, and $T_0=\bigcup_{n\geq 1}\Psi_n$ is the set of all wet instants in the history of the column. Moreover, let X_t^1 denote the amount of moisture *contained* in the column at any given dry instant $t\in T_1$, and let X_t^0 denote

the amount of moisture *contained* in the column at any given wet instant $t \in T_0$. Then, according to the model suggested by FP, the evolution of the column's moisture content in the course of time is modeled as a *piece-wise glued diffusion* process formulated in terms of the stochastic differential equations

$$\dot{X}_t^1 = \mu + \beta_1 \cdot \dot{W}_t \quad , \qquad t \in T_1 \qquad (1)$$

$$\dot{X}_t^0 = \mu - \rho + \beta_0 \cdot \dot{W}_t \quad , \quad t \in T_0 \qquad (2)$$

driven by a standard Wiener process $W = \{W_t ; t \geq 0\}$. The parameter $\mu > 0$ denotes the net rate of moisture converging into the column, the parameter $\rho > \mu > 0$ denotes the rate of precipitation produced by the column when it rains, and both parameters are treated, ideally, as being constants. Under this setting, the stochastic processes $X^1 = \{X_t^1 ; t \in T_1\}$ and $X^0 = \{X_t^0 ; t \in T_0\}$ are diffusions with constant drift coefficients $\mu > 0$ and $\mu - \rho < 0$ respectively, and also with constant diffusion coefficients $\beta_1 > 0$ and $\beta_0 > 0$. Equations (1) and (2) express a budget of the amount of moisture X_t contained in the column at any given instant $t \geq 0$ (dry or wet), taking into account the trade off between incoming moist air and outgoing moisture in the form of precipitated water. Under equation (1) the moisture content tends to grow due to the positive drift $\mu > 0$, while under equation (2) the moisture content tends to decay due to the negative drift $\mu - \rho < 0$.

A fine point in the conception of such a model is the assumption that there exist two critical thresholds of moisture content $0 < x_0 < x_1 < \infty$, of which the upper threshold x_1 is referred to as *saturation threshold*, and the lower one x_0 is referred to as *dehydration threshold*. The nomenclature associated with these two thresholds is justifiable in the following sense. During any dry epoch $\Phi_n = [\xi_{n-1}, \tau_n)$ the moisture

of the column is $X_t = X_t^1$, evolving as a diffusion with drift $\mu > 0$ according to (1), until it hits the saturation threshold x_1 from below. At that very instant τ_n the moisture content is $X_{\tau_n} = x_1$, the diffusion of equation (1) is killed, the column starts to precipitate, and the moisture content starts to evolve according to the diffusion of equation (2). That is, during the wet epoch $\Psi_n = [\tau_n, \xi_n)$ following precisely after the dry epoch Φ_n, the moisture content is $X_t = X_t^0$ until, due to the negative drift $\mu - \rho < 0$, the moisture content hits the dehydration threshold x_0 from above. At that very instant ξ_n, the moisture content is $X_{\xi_n} = x_0$, the diffusion of equation (2) is killed, the column stops precipitating, and equation (1) takes over anew to dictate the evolution of moisture content in the next dry epoch $\Phi_{n+1} = [\xi_n, \tau_{n+1})$. Thus, the sample paths of the *unconditional* moisture content process $\boldsymbol{X} = \{X_t ; t \geq 0\}$ are obtained by gluing together the sample paths of the conditional diffusion processes $\boldsymbol{X}^1 = \{X_t^1 ; t \in T_1\}$ and $\boldsymbol{X}^0 = \{X_t^0 ; t \in T_0\}$. The gluing operation occurs precisely at the killing boundary x_1 of X_t^1 when $t = \tau_n$, and at the killing boundary x_0 of X_t^0 when $t = \xi_n$, for every $n \geq 1$.

As pointed out by FP, the above model captures the intermittent behavior of rainfall by means of a hysteresis effect. That is, once rainfall starts at an instant τ_n where the moisture hits the saturation threshold x_1, it will continue raining until the moisture hits the dehydration level x_0, after eventually several up-crossings and down-crossings of x_1. Similarly, once rainfall stops at an instant ξ_n where the moisture hits the dehydration level x_0, it will remain stopped until the moisture hits the saturation threshold x_1, after eventually several down-crossings and up-crossings

of x_0. Another consequence of the model, pointed out by FP, is that the dry epoch durations $\{\phi_n\}_{n\geq 1}$ and the wet epoch durations $\{\psi_n\}_{n\geq 1}$ are both sequences of *independent and identically distributed (i.i.d.)* random variables, due to the positive recurrence of the diffusions described by the equations (1) and (2) ; see Bhattacharya and Waymire (1990). Moreover, it is also a well known probabilistic fact - see Karlin and Taylor (1975) - that the common probability distribution of each one of these two sequences of i.i.d. random variables belongs to the family of inverse Gaussian probability distributions. The probability density function of an inverse Gaussian distribution involves only two parameters $m>0$ and $l>0$, and is given by the formula ; see Johnson and Kotz (1970)

$$\pi(s)=\sqrt{\frac{l}{2\pi\cdot s^3}}\cdot\exp\left\{-\frac{l\cdot(s-m)^2}{2m^2\cdot s}\right\},\ s>0 \qquad (3)$$

According to FP, the probability density functions of dry and wet epoch durations, expressed in terms of the model's parameters are given, respectively, by

$$\pi_\phi(s)=\frac{x_1-x_0}{\beta_1\cdot\sqrt{2\pi\cdot s^3}}\cdot\exp\left\{-\frac{1}{2\beta_1^{\,2}\cdot s}\cdot\left[(x_1-x_0)-\mu\cdot s\right]^2\right\},\ s>0 \quad (4),$$

$$\pi_\psi(s)=\frac{x_1-x_0}{\beta_0\cdot\sqrt{2\pi\cdot s^3}}\cdot\exp\left\{-\frac{1}{2\beta_0^{\,2}\cdot s}\cdot\left[(x_1-x_0)-(\rho-\mu)\cdot s\right]^2\right\},\ s>0 \quad (5).$$

Indeed, both (4) and (5) are reducible to the standard inverse Gaussian probability density function (3) by using the corresponding reparametrization for

$$\underline{\text{Dry Phase}} \qquad m_\phi=\frac{x_1-x_0}{\mu} \quad l_\phi=\left(\frac{x_1-x_0}{\beta_1}\right)^2,$$

$$\underline{\text{Wet Phase}} \qquad m_\psi=\frac{x_1-x_0}{\rho-\mu} \quad l_\psi=\left(\frac{x_1-x_0}{\beta_0}\right)^2.$$

Thus, the stochastic model for budget of moisture introduced by FP, leads to explicit inverse Gaussian probability laws governing the durations of dry and wet epochs. Moreover, the parameters involved $x_1 - x_0, \rho, \mu, \beta_1, \beta_0$, are all physically interpretable, and also estimable (see FP for more details). For these reasons it is a rather worthy task to compare the goodness of fit of inverse Gaussian Laws against that of lognormal laws, regarding real data of dry and wet epoch durations. This very task shall be carried out in Section 4, while in Section 3 the i.i.d. hypotheses for dry and wet epoch durations shall be tested.

2.3 The Candidacy of Gamma Distribution

So far, in this section, some motivation has been reasoned regarding the candidacy of the lognormal and inverse Gaussian probability laws as plausible models for the probability distribution of wet and dry epoch durations.

However, before proceeding to the quantitative comparison of these two candidates with respect to their goodness of fit to real data, it is interesting to contemplate on the possibility of a third candidate, namely the Gamma probability law.

In a series of review papers on the mathematical structure of rainfall representations, Waymire and Gupta (1981a, 1981b, 1981c) gave quite a thorough summary of the efforts made by researchers (hydrologists, meteorologists, mathematicians) to model the structure of rainfall in time and space.

From that review it becomes evident that the main stream of rainfall modeling, in a time span of nearly two decades, was dominated by point process type of models. This fact may be attributed to the very influential work of LeCam (1961)

on the subject. Since then, other approaches have emerged more recently, based on multiplicative random cascades (see Gupta and Waymire (1990, 1993)) or models based on diffusion type of processes (see Pavlopoulos and Kedem (1992)). Nevertheless, point process type of models, regarding both temporal and spatial aspects of rainfall structure, remain to be a rather popular and valid approach.

In a most simple minded point process type of approach to modeling the temporal structure of rainfall, the number of occurrences of rainfall events may be modeled in terms of Poisson counting processes. Under such a model, the durations of wet and dry epochs will follow exponential probability distributions with different parameters; see Crovelli (1971) and Eagleson (1978). Since exponential distributions are special cases of Weibull and of Gamma distributions, it is conceivable that the probability distributions of dry and wet epoch durations may be more adequately modeled by these more general families of probability distributions, namely the Weibull or the Gamma family. In fact, Grayman and Eagleson (1971) did fit Weibull distributions to data of dry and wet epoch durations obtained from rainfall records in units of 10-minute increments. In the same work, Grayman and Eagleson (1971) investigated the stochastic dependence between the duration and the total intensity of rainfall per storm, and developed regression relations between these two variables. Motivated by this work, Crovelli (1971) introduced a bivariate gamma density as a model for the joint probability distribution between duration and magnitude of rainfall.

In light of this history, it is of interest to investigate the goodness of fit of Gamma distributions to the lengths of dry and wet spells of spatially averaged rain intensity. This task will be executed in the fourth section, along with a comparison of

the fits among the three candidate distributions, Lognormal, inverse Gaussian, and Gamma.

A similar comparison between Lognormal, Inverse Gaussian, and Gamma distribution tails has been made by Short, Shimizu, and Kedem (1993) regarding their fit to data of area averaged rain rate. In particular, it has been shown conditionally on large values, that Lognormal gives very high variability, Inverse Gaussian much less, and Gamma gives the least. This tail behavior distinguishes between the three distributions.

CHAPTER 3

DATA AND TESTING FOR RANDOMNESS

3.1 Description of the Data

The data which shall be used in this dissertation are a small portion of a data set of rain rate measurements collected during a 21 day period (December 20, 1992 through January 9, 1993) known as Cruise 2 of the Intensive Observing Period (IOP) of the Tropical Ocean Global Atmosphere (TOGA) Coupled Ocean-Atmosphere Response Experiment (COARE).

The measurements were obtained from two Doppler precipitation radars, which were *scanning every ten (10) minutes* a large tropical region in the China Sea, of approximate size 300 km×400 km, located at 2° South and 156° East. The two radars, named TOGA and MIT, were on board the ships R/V Xiangyanghong#5 (Peoples' Republic of China) and R/V JV Vickers (U.S.A), respectively. Rain rates were obtained from the reflectivities of each radar snapshot, which then were binned over small pixels of size 2×2 km^2 each.

The used data set consists of five synchronous time series of instantaneous spatial averages of rain rate over fixed sub-regions of sizes: a) 10×10 km^2 (5×5 pixels), b) 8×8 km^2 (4×4 pixels), c) 6×6 km^2 (3×3 pixels), d) 4×4 km^2 (2×2 pixels), e) 2×2 km^2 (1×1 pixel), which lied within the intersection of the ranges of the two radars. Moreover, each sub-region is nested inside all the ones which are larger in size. This means, that each measurement in each of the five synchronous series, corresponds to a different single snapshot and it is the average of 25, or 16, or 9, or 4,

or 1 values of rain rate obtained from the binned reflectivities over the corresponding 25, 16, 9, 4, 1 contiguous pixels of the snapshot.

Blocks of zeros and blocks of positive spatial averages, appearing in alternating sequence in each of the five time series, correspond to the dry and wet phases respectively. The dry and wet epoch durations are estimated by the corresponding number of measurements in a given block multiplied *by 10 minutes*. The TOGA-COARE data base consists of 3024 snapshots. However, each of the above five time series is shorter by 28 which are missing. Those 28 missing observations were identified with respect to their time coordinate and they appeared in each time series in a formation of 11 blocks. This means that some blocks of zero or positive measurements border with a block of missing measurements, yielding just a few dry or wet phases of ambiguous length. In order to avoid this kind of problem, those blocks (of zeros or of positive measurements) which border with blocks of missing values, have been discarded. After this censoring operation, the numbers of dry and wet blocks have been counted for each of the five time series, and they are tabulated in Table 1.

TABLE 1		
TIME SERIES	DRY	WET
5×5 pixels, 10×10 km^2	172	175
4×4 pixels, 8×8 km^2	162	167
3×3 pixels, 6×6 km^2	149	154
2×2 pixels, 4×4 km^2	153	159
1×1 pixels, 2×2 km^2	138	144

Table 1. Numbers of dry and wet blocks of the time series which correspond to the five area sizes.

Explicit information about the lengths of dry and wet durations, in units of hours, for each one of the five nested regions, is given in the Tables A-J of the Appendix.

3.2 Testing Randomness

In Section 2, it was pointed out that, according to the model introduced by Freidlin and Pavlopoulos (1997), the durations of dry and wet epochs must be sequences of i.i.d. random variables. In order to test the validity of this point, for processes of spatially averaged rain rate, a certain ramification of the well known Wald-Wolfowitz test, based on the number of runs above and below the median, is employed (see Brownlee (1965)). Given a sample of observations from a continuous parent probability distribution, each observation is replaced by the symbol A or B according to whether it is greater than (above) or less than (below) the median of the sample. In this labeling process, observations which coincide with the median are discarded from the sample. The result of this operation is a sequence of type AA BB AA BBB A BBB AAA BBB , for example. Then, the total number n_1 of A's, the total number n_2 of B's, and the total number U of runs of like elements are computed. In the above example, n_1=8, n_2=11, and U=8, since there is a total of 8 runs (underlined strings of labels).

If n_1 and n_2 are both large enough scores (i.e. larger than 10), then under the null hypothesis that the sample consists of i.i.d. observations, the probability distribution of U is well approximated by a normal law with mean and variance given by (Wolfowitz (1944)):

$$\mu_u = \frac{2n_1n_2}{n_1+n_2}+1 \ , \ \sigma_u^2 = \frac{2n_1n_2\left(2n_1n_2-n_1-n_2\right)}{\left(n_1+n_2\right)^2\left(n_1+n_2-1\right)}.$$

It is worth noting that this asymptotic result makes no further assumptions about the parent distribution of the sample, except that it is of continuous type, which is to say that it establishes a non-parametric test. Including a continuity correction, suggested by Wallis (1952), the test rejects the null hypothesis of randomness (i.i.d.) if the absolute value of the statistic

$$Z = \frac{U-\mu_u+0.5}{\sigma_u},$$

exceeds a specified percentile of the standard normal distribution. Namely, at the $0<\alpha<1$ level of significance, the null hypothesis is rejected if $|Z| \geq Z_{1-\frac{\alpha}{2}}$, where $Z_{1-\frac{\alpha}{2}}$ is the $(1-\alpha/2)100\%$ percentile of the normal law N(0, 1).

This non-parametric test is applied to the observed samples of dry and of wet durations, separately for each area size in the following two subsections.

3.2.1 Dry Spells

Table 2, summarizes the information of the above test, applied to sequences of dry durations for each one of the examined area sizes.

TABLE 2. DRY SEQUENCES

AREA	MEDIAN (HOURS)	OBSERVATIONS ABOVE THE MEDIAN (n_1)	OBSERVATIONS BELOW THE MEDIAN (n_2)	RUNS (U)	MEAN OF RUNS (μ_U)	VARIANCE OF RUNS (σ^2_U)	TEST STATISTIC (Z)	P-VALUE TWO SIDED
10×10 km²	0.6667	76	82	75	79.8861	39.1346	-0.7011	0.4832
8×8 km²	0.6667	79	72	69	76.3377	37.3363	-1.119	0.2632
6×6 km²	0.6667	71	68	71	70.4676	34.4658	0.1759	0.8604
4×4 km²	0.6667	75	72	63	74.4694	36.4677	-1.8165	0.0693
2×2 km²	0.8333	66	65	53	66.4962	32.4943	-2.2798	0.0226

Table 2. Results obtained after the application of the Runs test to the dry sequences.

It is clearly seen that, as the size of the area decreases, the hypothesis that the sequence of dry durations is an i.i.d. sequence *tends to be not valid.* In other words, there is no ample evidence to support the null hypothesis, except in the case of 6×6 km^2. We note that the smallest p-value 2.26% corresponds to the smallest area (2×2 km^2), and the largest p-value corresponds to the intermediate size area (6×6 km^2). Nevertheless, at 1% level of significance we cannot reject the null hypothesis, regardless of the area size.

3.2.2 Wet Spells

Table 3, tabulates the information regarding the results of applying the runs test above and below the median to the sequences of wet durations, corresponding to the five examined area sizes.

TABLE 3. WET SEQUENCES

AREA	MEDIAN (HOURS)	OBSERVATIONS ABOVE THE MEDIAN (n_1)	OBSERVATIONS BELOW THE MEDIAN (n_2)	RUNS (U)	MEAN OF RUNS (μ_U)	VARIANCE OF RUNS (σ^2_U)	TEST STATISTIC (Z)	P-VALUE TWO SIDED
10×10 km^2	0.5	75	84	72	80.2453	39.2441	-1.2364	0.2162
8×8 km^2	0.5	70	83	78	76.9477	37.4481	0.2537	0.7998
6×6 km^2	0.5	70	72	65	71.9859	35.2341	-1.0927	0.2746
4×4 km^2	0.5	59	79	60	68.5507	32.8142	-1.4054	0.1598
2×2 km^2	0.3333	61	58	56	60.4622	29.4601	-0.7299	0.4654

Table 3. Results obtained after the application of the Runs test to the wet sequences.

It is clearly seen here that the null hypothesis cannot be rejected considering 1%, 5%, and 10% levels of significance for each one of the sub-region sizes. The smaller estimated two sided p-value is 15.98% (4×4 km^2 region) while the larger is 79.98% (8×8 km^2 region). Thus, there is enough evidence to support the i.i.d. hypothesis for sequences of wet epoch duration.

CHAPTER 4

ESTIMATION AND GOODNESS OF FIT

4.1 Estimation of Parameters

This section deals with the estimation of parameters of the Lognormal, Inverse Gaussian, and Gamma models, for dry and wet phases.

Given the standard form of the Lognormal density

$$\frac{1}{\sigma x\sqrt{2\pi}} \cdot \exp\left\{-\frac{1}{2}\cdot\left(\frac{\log x-\mu}{\sigma}\right)^2\right\},\ x>0,\ \mu\in R,\ \sigma>0$$

the maximum likelihood estimators (MLE) of the parameters are (Johnson and Kotz (1970))

$$\hat{\mu}=\frac{\sum_{i=1}^{n}\log x_i}{n}\quad,\qquad \hat{\sigma}^2=\frac{\sum_{i=1}^{n}\left(\log x_i-\hat{\mu}\right)^2}{n},$$

and the method of moments estimators (MME) are

$$\tilde{\mu}=\log\left(\left(\sum_{i=1}^{n}x_i\right)^2\Big/\left(n^3\sum_{i=1}^{n}x_i^2\right)^{\frac{1}{2}}\right)\quad,\qquad \tilde{\sigma}^2=\log\left(n\sum_{i=1}^{n}x_i^2\Big/\left(\sum_{i=1}^{n}x_i\right)^2\right).$$

Given the standard form of the Inverse Gaussian density

$$\sqrt{\frac{l}{2\pi\cdot x^3}}\cdot\exp\left\{-\frac{l}{2m^2\cdot x}\cdot(x-m)^2\right\},\ x>0,\ l>0,\ m>0$$

the MLE of the parameters are (Johnson and Kotz (1970))

$$\hat{m} = \bar{x} = \frac{\sum_{i=1}^{n} x_i}{n}, \qquad \hat{l} = \left[\frac{1}{n} \sum_{i=1}^{n} \left(\frac{1}{x_i} - \frac{1}{\bar{x}} \right) \right]^{-1},$$

and the MME are

$$\tilde{m} = \bar{x}, \qquad \tilde{l} = \left[\frac{\frac{1}{n} \sum_{i=1}^{n} x_i^2}{\bar{x}^3} - \frac{1}{\bar{x}} \right]^{-1},$$

and note that $\tilde{m} = \bar{x} = \hat{m}$.

Finally, given the standard form of the Gamma density

$$\frac{1}{\beta^{\alpha} \Gamma(\alpha)} \cdot x^{\alpha - 1} \cdot \exp\left\{ - \frac{x}{\beta} \right\}, \; x > 0, \; \alpha > 0, \; \beta > 0,$$

the MLE are approximated (Johnson and Kotz (1970)) by

$$\hat{\alpha} \cong \frac{1}{4} Y^{-1} \left(1 + \sqrt{1 + \frac{4}{3} Y} \right), \qquad \hat{\beta} \cong \frac{\bar{X}}{\hat{\alpha}}$$

where $Y = \log(\bar{x}) - \frac{1}{n} \log\left(\prod_{i=1}^{n} x_i \right)$, and the MME are

$$\tilde{\alpha} = \frac{\left(\sum_{i=1}^{n} X_i \right)^2}{n \sum_{i=1}^{n} X_i^2 - \left(\sum_{i=1}^{n} X_i \right)^2}, \qquad \tilde{\beta} = \frac{n \sum_{i=1}^{n} X_i^2 - \left(\sum_{i=1}^{n} X_i \right)^2}{n \sum_{i=1}^{n} X_i}.$$

Tables 4 and 5, corresponding to dry and wet phases, provide the estimates of the parameters (MLE, MME) of the three distributions obtained from the analyzed five time series. For each time series (appearing under TS on both tables where TS 1, TS 2, TS 3, TS 4 & TS 5 correspond to the areas 2×2 km^2, 4×4 km^2, 6×6 km^2, 8×8 km^2, 10×10 km^2, respectively), the parameters of Lognormal, Inverse Gaussian and Gamma distributions, respectively, have been estimated. For example, for the dry phases (Table 4), referring to the time series TS 1 (scanned area 2×2 km^2), the Lognormal MLE are μ=-0.1075 and σ^2=1.7779; the Inverse Gaussian MME are m=2.157 and l=0.882, and finally the Gamma MME are α=0.4089 and β=5.2749.

TABLE 4												
DRY												
LOGNORMAL					INVERSE GAUSSIAN				GAMMA			
	μ		σ^2		m		l		α		β	
TS	MLE	MME	MLE	MME	MLE	MME	MLE	MME	MLE	MME	MLE	MME
1	-0.1075	0.1502	1.7779	1.2371	2.157	2.157	0.5599	0.882	0.7054	0.4089	3.0579	5.2749
2	-0.2427	0.0475	1.6771	1.08	1.7995	1.7995	0.5298	0.9253	0.7382	0.5142	2.4376	3.4995
3	-0.2202	0.0395	1.5877	1.0699	1.7763	1.7763	0.5666	0.9274	0.7659	0.5221	2.3192	3.4021
4	-0.2903	-0.0822	1.4344	1.0094	1.5257	1.5257	0.5757	0.8748	0.8405	0.5734	1.8152	2.6607
5	-0.3816	-0.1789	1.4478	1.0613	1.4215	1.4215	0.5284	0.752	0.8204	0.529	1.7327	2.6869

Table 4. Lognormal, Inverse Gaussian and Gamma parameters of Dry phases for each time series.

TABLE 5												
WET												
LOGNORMAL					INVERSE GAUSSIAN				GAMMA			
	μ		σ^2		m		l		α		β	
TS	MLE	MME	MLE	MME	MLE	MME	MLE	MME	MLE	MME	MLE	MME
1	-0.8405	-0.7746	0.9951	1.0075	0.7627	0.7627	0.4856	0.4386	1.0211	0.5751	0.7469	1.3262
2	-0.7418	-0.6935	0.9988	1.0323	0.8375	0.8375	0.5256	0.4633	1.0293	0.5532	0.8137	1.5139
3	-0.5899	-0.4843	1.1009	0.9446	0.9881	0.9881	0.5556	0.6286	1.0082	0.6362	0.98	1.5531
4	-0.6425	-0.5542	1.1537	1.1183	1.005	1.005	0.5099	0.4879	0.9133	0.4855	1.1004	2.0699
5	-0.6276	-0.5136	1.2173	1.1203	1.0476	1.0476	0.4938	0.5071	0.882	0.4841	1.1877	2.1639

Table 5. Lognormal, Inverse Gaussian and Gamma parameters of Wet phases for each time series.

4.2 Tests and Comparison of Goodness of Fit

In this section the goodness of fit of each of the three distributions (Gamma, Inverse Gaussian, Lognormal) is tested by using the well known χ^2 -statistic defined by

$$\chi^2 = \sum_{i=1}^{k} \frac{\left(O_i - E_i(\hat{\vartheta})\right)^2}{E_i(\hat{\vartheta})},$$

where k is the number of groups into which the data are partitioned, O_i is the number of observations belonging to the i-th group, $E_i(\hat{\vartheta})$ is the expected number of observations in the i-th group, under the null hypothesis, and $\hat{\vartheta}$ is the vector of the estimates of the parameters ϑ of the probability distribution which is tested under the null hypothesis.

It is a well known fact (Cramer, (1974)) that the probability distribution of the χ^2 statistic is approximately a χ^2_{k-h-1} distribution with (k-h-1) degrees of freedom,

where h is the number of the estimated parameters. The goodness of fit of each distribution is simply judged by how small is the value of the χ^2 statistic and also by how large is the corresponding P-value of the test.

Clearly, for the Lognormal distribution $\vartheta=(\mu, \sigma^2)$, for the Inverse Gaussian case $\vartheta=(m, l)$, and for the Gamma case $\vartheta=(\alpha, \beta)$. In all three cases, h is equal to two, and therefore the degrees of freedom of approximate Chi-Square distribution are k-3.

In the cases where the expected number of observations in the last group $E_i(\hat{\vartheta})$ are less than five, these frequencies have been included in the very previous group, so as to obtain $E_i(\hat{\vartheta})$ greater than five (see also Peters and Summers (1968), Yamane (1973)). In each such case, the grouping of the observed data is modified in the same way, and therefore the number of degrees of freedom (DF) of the Chi-Square distribution is reduced by one (see Tables 6-10, and Tables 11-15).

It is important to note that, due to the fixed sampling frequency of one snapshot in every 10 minutes (or 0.1667 hours) by the radar, the data sets of dry and wet durations do not include any values less than 0.1667 hours. Thus, it is appropriate, instead of fitting the *standard* densities, to fit the *truncated* versions at 0.1667 hours. In general, the truncated fitted density is given by $\frac{f(w)}{\int_q^\infty f(w)dw}$ (see for example Kedem et al. (1990)), where f(.) in our case is one of the Lognormal, Inverse Gaussian, or Gamma *standard* densities, and q= 0.1667. For example, for the dry data, the truncated fitted Inverse Gaussian densities are (for MLE, MME respectively)

$$\frac{\hat{f}_{IG,\,dry}(x)}{\int_{0.1667}^{\infty}\hat{f}_{IG,\,dry}(x)dx}\,,\quad \frac{\tilde{f}_{IG,\,dry}(x)}{\int_{0.1667}^{\infty}\tilde{f}_{IG,\,dry}(x)dx}\,.$$

It is also noted that, for the Lognormal distribution, the calculation of the integrals of the density is direct via the relation

$$\int_{g}^{j}\frac{1}{x\sigma\sqrt{2\pi}}\exp\left\{-\frac{1}{2}\left(\frac{\log x-\mu}{\sigma}\right)^{2}\right\}dx=\Phi\left(\frac{\log(j)-\mu}{\sigma}\right)-\Phi\left(\frac{\log(g)-\mu}{\sigma}\right),$$

where Φ is the cumulative distribution function of the standard normal distribution N(0,1). On the other hand, for the Inverse Gaussian and the Gamma case, the integrals have been calculated via numerical integration.

All the information obtained from the fits of MME and MLE estimates of the Lognormal, inverse Gaussian, and Gamma densities to data of dry and wet epoch durations, is summarized in tables given in the following two sub-sections. The first column of the table, named classes, for each time series (that is, for each size of the area), contains the endpoints of the intervals into which the data were grouped (i.e. for the 2×2 km^2 area of dry phases, we have [0.1667-1.25), [1.25-2.15), [2.15-2.8), [2.8-4), [4-6), [6-9.5), [9.5-∞), in units of hours). The second column contains the observed frequencies of the data (durations falling into i-th class). The fitted frequencies correspond to Lognormal, Inverse Gaussian and Gamma densities, truncated at 0.1667 (either MLE or MME). Also, the values of the Chi-Square statistic, the corresponding P-values and the degrees of freedom (DF) are tabulated. We separately examine the fitting for either the dry or the wet phase, respectively, in the following two subsections.

4.2.1 Dry Epoch Duration

In this subsection, the next five tables (Tables 6-10) summarize the information regarding the fits of the densities, for each case of the examined area size.

1st) Smaller area (2×2 km^2)

TABLE 6								
2×2 KM^2			*FITTED*					
			LOGNORMAL		*INVERSE GAUSSIAN*		*GAMMA*	
CLASSES		*FREQUENCIES*	*MLE*	*MME*	*MLE*	*MME*	*MLE*	*MME*
0.1667	1.25	79	76.1212	69.8539	82.6215	76.8539	57.5537	59.443
1.25	2.15	19	22.4299	26.4314	18.8869	22.199	25.217	21.4654
2.15	2.8	8	9.1487	10.8585	7.5863	8.9734	12.5572	10.5908
2.8	4	9	10.0942	11.7005	8.5728	10.0051	15.7184	13.6832
4	6	10	8.3298	9.092	7.5393	8.4713	14.0661	13.5246
6	9.5	6	5.9593	5.8302	5.9973	6.2305	9.1899	11.08
9.5	∞	7	5.9168	4.2334	6.7957	5.2668	3.6977	8.2128
TOTAL		138	138	138	138	138	138	138
CHISQUARE			**1.4297**	**5.6101**	**1.01249**	**1.5822**	**15.226**	**12.381**
P -VALUE			**0.839**	**0.1322**	**0.9079**	**0.812**	**0.0016**	**0.0147**
DF			**4**	**3**	**4**	**4**	**3**	**4**

Table 6. Goodness of fit of the three probability models for dry durations corresponding to 2×2 km^2 area.

2nd) Small area (4×4 km^2)

TABLE 7								
4×4 KM^2			*FITTED*					
			LOGNORMAL		*INVERSE GAUSSIAN*		*GAMMA*	
CLASSES		*FREQUENCIES*	*MLE*	*MME*	*MLE*	*MME*	*MLE*	*MME*
0.1667	1.3	95	92.734	86.477	97.679	91.75	73.042	73.5168
1.3	2.4	24	26.704	32.664	22.733	27.812	33.4287	29.8423
2.4	3.17	9	9.2581	11.018	8.0432	9.6727	14.1503	12.901
3.17	4.9	10	10.704	11.868	9.851	11.267	17.679	17.2381
4.9	9	9	8.4472	7.9029	8.7751	8.7445	12.2852	14.6417
9	∞	6	5.1524	3.0692	5.9189	3.7534	2.41487	4.8601
TOTAL		153	153	153	153	153	153	153
CHISQUARE			**0.5583**	**5.2806**	**0.2671**	**1.328**	**14.4765**	**12.6796**
P -VALUE			**0.9059**	**0.0713**	**0.9661**	**0.5148**	**0.00072**	**0.00176**
DF			**3**	**2**	**3**	**2**	**2**	**2**

Table 7. Goodness of fit of the three probability models for dry durations corresponding to 4×4 km^2 area.

3rd) Medium area (6×6 km^2)

TABLE 8								
6×6 KM^2			*FITTED*					
			LOGNORMAL		*INVERSE GAUSSIAN*		*GAMMA*	
CLASSES		*FREQUENCIES*	*MLE*	*MME*	*MLE*	*MME*	*MLE*	*MME*
0.1667	1.5	99	97.3648	92.9504	100.775	96.7782	79.2059	78.8443
1.5	2.35	17	18.8178	22.6748	16.0746	19.2834	24.2714	21.4751
2.35	3.2	9	10.1256	11.888	8.8819	10.4664	15.4088	13.9828
3.2	5.1	10	10.8433	11.8553	10.1795	11.3863	17.8325	17.5805
5.1	8.1	7	6.3051	5.9716	6.6499	6.62	9.1863	11.0955
8.1	∞	7	5.5436	3.6599	6.4392	4.4657	3.0951	6.02185
TOTAL		149	149	149	149	149	149	149
CHISQUARE			**0.85297**	**4.78727**	**0.15654**	**1.46179**	**13.4714**	**12.8**
P -VALUE			**0.83676**	**0.0913**	**0.98428**	**0.48148**	**0.00119**	**0.00509**
DF			**3**	**2**	**3**	**2**	**2**	**3**

Table 8. Goodness of fit of the three probability models for dry durations corresponding to 6×6 km^2 area.

4th) Large area (8×8 km^2)

TABLE 9								
8×8 KM^2			*FITTED*					
			LOGNORMAL		*INVERSE GAUSSIAN*		*GAMMA*	
CLASSES		*FREQUENCIES*	*MLE*	*MME*	*MLE*	*MME*	*MLE*	*MME*
0.1667	1.3	104	103.671	99.9817	107.193	103.775	85.168	84.6623
1.3	2.1	21	23.1434	27.0897	20.0784	23.3393	29.5781	26.2036
2.1	2.9	11	11.8434	13.4281	10.6017	12.0662	17.8669	16.3779
2.9	4.1	9	9.2710	9.8683	8.8173	9.5929	14.8079	14.7198
4.1	6	8	6.6367	6.3636	6.8898	6.9049	9.6967	11.3264
6	∞	9	7.4344	5.2686	8.4199	6.3211	4.8824	8.7102
TOTAL		162	162	162	162	162	162	162
CHISQUARE			**0.87729**	**5.10939**	**0.37501**	**1.67476**	**11.9709**	**10.4253**
P -VALUE			**0.83091**	**0.16396**	**0.94536**	**0.64256**	**0.00252**	**0.01528**
DF			**3**	**3**	**3**	**3**	**2**	**3**

Table 9. Goodness of fit of the three probability models for dry durations corresponding to 8×8 km^2 area.

5th) Larger area (10×10 km^2)

TABLE 10								
10×10 KM²			*FITTED*					
			LOGNORMAL		*INVERSE GAUSSIAN*		*GAMMA*	
CLASSES		*FREQUENCIES*	*MLE*	*MME*	*MLE*	*MME*	*MLE*	*MME*
0.1667	1	102	98.5383	93.2288	102.926	99.0644	77.2807	77.7168
1	1.5	19	23.2853	26.6411	20.3559	22.8994	26.5222	23.2252
1.5	2	12	13.8178	15.8314	12.1189	13.6263	18.6728	16.4051
2	2.5	9	8.9003	10.0084	8.0187	8.8990	13.3926	12.0734
2.5	3.1	7	7.0557	7.7051	6.6019	7.1790	11.2482	10.6679
3.1	4.5	10	8.9509	9.2352	8.9459	9.3301	14.3232	15.1148
4.5	6.5	6	5.4750	5.0990	6.0349	5.7994	7.4043	9.7924
6.5	∞	7	5.9767	4.2509	6.9979	5.2023	3.1559	7.0044
TOTAL		172	172	172	172	172	172	172
CHISQUARE			**1.49944**	**5.59836**	**0.36829**	**1.62697**	**17.3385**	**14.782**
P-VALUE			**0.91313**	**0.23122**	**0.99616**	**0.89797**	**0.00166**	**0.01134**
DF			**5**	**4**	**5**	**5**	**4**	**5**

Table 10. Goodness of fit of the three probability models for dry durations corresponding to 10×10 km^2 area.

Overall, we note that MLE fit better than MME, for each distribution model. Examining carefully the above tables of the durations of the dry epochs, from smaller to larger area sizes, we can clearly see that *the fitting which corresponds to Inverse Gaussian distribution is significantly better than the one obtained by the Lognormal distribution, for all the sizes of the areas*. More specifically, the results are almost *perfect* considering either the Chisquare values or the p-values of the IG fits. For the MLE, the p-values have range from 90.79% (size 2×2 km^2, Table 6) to 99.616% (size 10×10 km^2, Table 10). Also, dramatically better are the fits of MME IG densities than the fits of MME LN densities. The fitting that corresponds to Gamma distribution is clearly very *poor* for all the area sizes, for both MME or MLE.

All the above suggest that the Inverse Gaussian is a better model than Lognormal and Gamma distributions for dry durations of spatially averaged rain rate. On the other hand, Gamma appears to be a most inadequate model for dry epoch durations.

4.2.2 Wet Epoch Duration

This subsection deals with the fitting of the three distributions (Inverse Gaussian, Lognormal and Gamma) which correspond to the wet durations. The next five tables (Tables 11-15) summarize all the information needed for this comparison.

1st) Smaller area (2×2 km^2)

TABLE 11								
2×2 KM²			*FITTED*					
			LOGNORMAL		*INVERSE GAUSSIAN*		*GAMMA*	
CLASSES		*FREQUENCIES*	*MLE*	*MME*	*MLE*	*MME*	*MLE*	*MME*
0.1667	1	109	109.341	106.4649	105.935	105.511	95.9519	89.0336
1	1.35	12	12.7201	13.2982	12.4995	12.2396	17.8467	15.9124
1.35	2.05	11	11.6801	12.5542	12.5885	12.4994	18.2936	18.6
2.05	2.9	6	5.3877	5.9814	6.5624	6.6901	8.0696	10.7783
2.9	∞	6	4.8706	5.7012	6.4148	7.0599	3.8382	9.67578
TOTAL		144	144	144	144	144	144	144
CHISQUARE			**0.3771**	**0.39522**	**0.3841**	**0.53**	**6.598**	**12.06**
P-VALUE			**0.5391**	**0.82069**	**0.8253**	**0.767**	**0.01**	**0.002**
DF			**1**	**2**	**2**	**2**	**1**	**2**

Table 11. Goodness of fit of the three probability models for wet durations corresponding to 2×2 km^2 area.

2nd) Small area (4×4 km^2)

TABLE 12								
4×4 KM^2			*FITTED*					
			LOGNORMAL		*INVERSE GAUSSIAN*		*GAMMA*	
CLASSES		*FREQUENCIES*	*MLE*	*MME*	*MLE*	*MME*	*MLE*	*MME*
0.1667	1.15	123	123.81	120.906	120.39	119.853	110.2205	101.894
1.15	1.7	15	16.285	16.9958	16.1675	15.7722	23.7679	21.4794
1.7	2.35	9	8.6395	9.302	9.4802	9.4316	13.6791	14.6087
2.35	3.25	6	5.1779	5.7536	6.3022	6.4553	7.5544	10.5838
3.25	∞	6	5.0925	6.0428	6.6596	7.48748	3.7782	10.4342
TOTAL		159	159	159	159	159	159	159
CHISQUARE			**0.4139**	**0.2913**	**0.24502**	**0.46779**	**6.3559**	**12.3495**
P-VALUE			**0.8131**	**0.86446**	**0.8847**	**0.79144**	**0.01169**	**0.00208**
DF			**2**	**2**	**2**	**2**	**1**	**2**

Table 12. Goodness of fit of the three probability models for wet durations corresponding to 4×4 km^2 area.

3rd) Medium area (6×6 km^2)

TABLE 13								
6×6 KM^2			*FITTED*					
			LOGNORMAL		*INVERSE GAUSSIAN*		*GAMMA*	
CLASSES		*FREQUENCIES*	*MLE*	*MME*	*MLE*	*MME*	*MLE*	*MME*
0.1667	1	103	103.427	101.72	103.419	103.187	87.782	84.876
1	1.6	21	23.044	24.699	21.2247	22.0051	30.23	26.676
1.6	2.35	13	12.6666	13.34	12.5213	12.7936	19.209	18.584
2.35	4.4	13	10.601	10.593	11.8144	11.6255	14.699	18.485
4.4	∞	4	4.26098	3.6441	5.0203	4.3886	2.0801	5.3789
TOTAL		154	154	154	154	154	154	154
CHISQUARE			**0.49943**	**1.1149**	**0.34873**	**0.11028**	**7.4659**	**8.7363**
P-VALUE			**0.47975**	**0.291**	**0.83999**	**0.73983**	**0.0063**	**0.0127**
DF			**1**	**1**	**2**	**1**	**1**	**2**

Table 13. Goodness of fit of the three probability models for wet durations corresponding to 6×6 km^2 area.

4th) Large area (8×8 km^2)

TABLE 14								
8×8 KM^2			*FITTED*					
			LOGNORMAL		*INVERSE GAUSSIAN*		*GAMMA*	
CLASSES		*FREQUENCIES*	*MLE*	*MME*	*MLE*	*MME*	*MLE*	*MME*
0.1667	1	126	126.081	123.09	123.13	123.05	109.24	101.983
1.25	2	19	20.1149	21.288	19.369	19.171	29.332	25.838
2	2.85	9	9.5432	10.285	10.25	10.209	15.594	16.1517
2.85	4.1	6	5.8186	6.3448	7.0198	7.0599	8.8163	12.0228
4.1	∞	7	5.4423	5.9961	7.2354	7.5111	4.0201	11.0048
TOTAL		167	167	167	167	167	167	167
CHISQUARE			**0.54425**	**0.6624**	**0.3823**	**0.4094**	**9.0012**	**15.107**
P-VALUE			**0.76176**	**0.7181**	**0.826**	**0.8149**	**0.0027**	**0.00052**
DF			**2**	**2**	**2**	**2**	**1**	**2**

Table 14. Goodness of fit of the three probability models for wet durations corresponding to 8×8 km^2 area.

5th) Larger area (10×10 km^2)

TABLE 15								
10×10 KM^2			*FITTED*					
			LOGNORMAL		*INVERSE GAUSSIAN*		*GAMMA*	
CLASSES		*FREQUENCIES*	*MLE*	*MME*	*MLE*	*MME*	*MLE*	*MME*
0.1667	1	120	116.672	113.056	115.4441	115.3777	95.4849	91.3892
1	1.5	18	22.5712	23.9183	20.5898	20.7446	28.8282	24.4389
1.5	2.1	12	13.7871	14.7761	13.3666	13.4454	20.9162	18.8169
2.1	2.8	8	8.3383	8.9535	8.7741	8.7999	13.6627	13.8624
2.8	4	7	6.6712	7.1252	7.7567	7.7427	10.4328	13.1436
4	6.2	5	4.2716	4.4895	5.5843	5.5245	4.8224	9.2929
6.2	∞	5	2.6882	2.6817	3.4845	3.3649	0.8527	4.0560
TOTAL		175	175	175	175	175	175	175
CHISQUARE			**2.61028**	**3.63213**	**0.88299**	**0.986382**	**20.9345**	**19.31419**
P-VALUE			**0.45569**	**0.30403**	**0.829531**	**0.804547**	**0.000109**	**0.000235**
DF			**3**	**3**	**3**	**3**	**3**	**3**

Table 15. Goodness of fit of the three probability models for wet durations corresponding to 10×10 km^2 area.

The results regarding the five above tables, which correspond to the wet phases of varying area sizes (from smaller to larger) are as follows:

a) The *superiority* of the Inverse Gaussian distribution fitting still holds versus the Lognormal one, considering the MLE. The p-values of IG have range from 88.47% (size area 4×4 km^2, Table 12) to 82.53% (size area 2×2 km^2, Table 11), while the p-values of LN are from 45.569% (size area 10×10 km^2, Table 15) to 81.31% (size area 4×4 km^2, Table 12) indicating that the hypotheses of IG and LN are not rejectable.

b) The fittings of both truncated versions of IG and LN for wet durations, are rather *not as good* as the ones obtained for the dry durations, where the p-values were larger than 90%, i.e. in the IG case.

c) The fits of the Gamma distribution model, as in the case of dry durations, indicate clearly that *the Gamma distribution is an inadequate model* for wet durations.

CHAPTER 5

SCALING EFFECTS

This section is concerned with the investigation of scaling of the moments with respect to the spatial scale, under both the IG and the LN model for dry and wet epoch durations, and also under no specific parametric model.

The values of the spatial scale λ in the case of the five nested sub-regions which have been considered in this work are: λ =1 (for 10×10 km^2), λ =0.8 (for 8×8 km^2), λ = 0.6 (for 6×6 km^2), λ =0.4 (for 4×4 km^2), and λ =0.2 (for 2×2 km^2).

It is well known (see Johnson & Kotz (1970)) that mean and variance for the Lognormal distribution LN(μ, σ^2) are given by the formulae:

$$M_{LOGNORMAL} = \exp\left\{\mu + \frac{\sigma^2}{2}\right\},$$

$$V_{LOGNORMAL} = \exp\{2\mu + \sigma^2\} \cdot \left[\exp\{\sigma^2\} - 1\right],$$

and for the Inverse Gaussian (m, l) distribution are given by

$$M_{INVERSE\ GAUSSIAN} = m,$$

$$V_{INVERSE\ GAUSSIAN} = \frac{m^3}{l}.$$

Table 16 tabulates MLE and MME estimates of M, V under the Lognormal and the Inverse Gaussian model for dry epoch durations.

Table 17 tabulates MLE and MME estimates of M, V under the Lognormal and Inverse Gaussian model for wet epoch durations.

TABLE 16. DRY DURATIONS								
AREA	SCALE λ	MEAN (LN)		VARIANCE (LN)		MEAN (IG)	VARIANCE (IG)	
		MLE	MME	MLE	MME	MLE=MME	MLE	MME
2×2 km^2	0.2	2.1846	2.1571	23.4691	11.3793	2.157	17.924	11.3784
4×4 km^2	0.4	1.8146	1.7995	14.3232	6.29715	1.7995	10.999	6.29757
6×6 km^2	0.6	1.7747	1.7762	12.2601	6.04157	1.7763	9.8917	6.04341
8×8 km^2	0.8	1.5325	1.5258	7.50862	4.05989	1.5257	6.1689	4.0597
10×10 km^2	1	1.4082	1.4216	6.45211	3.81959	1.4215	5.436	3.8196

Table 16. Lognormal and Inverse Gaussian mean and variance of dry durations.

TABLE 17. WET DURATIONS								
AREA	SCALE λ	MEAN (LN)		VARIANCE (LN)		MEAN (IG)	VARIANCE (IG)	
		MLE	MME	MLE	MME	MLE=MME	MLE	MME
2×2 km^2	0.2	0.7097	0.7627	0.8587	1.0115	0.7627	0.9137	1.01156
4×4 km^2	0.4	0.7847	0.8375	1.0561	1.2678	0.8375	1.1176	1.26792
6×6 km^2	0.6	0.9613	0.9881	1.8546	1.5345	0.9881	1.7364	1.53472
8×8 km^2	0.8	0.9365	1.005	1.9029	2.0801	1.005	1.9907	2.0805
10×10 km^2	1	0.9812	1.0477	2.2896	2.2673	1.0476	2.3283	2.26722

Table 17. Lognormal and Inverse Gaussian mean and variance of wet durations.

Table 16, corresponding to the DRY phases, shows that as the size of the area increases, the MME and MME means decrease under either the LN or the IG model. This behavior seems to be rather natural, because for larger areas, there is a larger number of pixels contributing to the persistence of rainfall. This suggests that the DRY durations become shorter as the area becomes larger. Moreover, this shortening has an effect of reducing also the variability of dry duration, which can indeed be seen in the decay of variances in Table 16 in all cases.

On the other hand, considering the WET phase durations in Table 17, it is seen that the mean of wet durations increases as the area size increases, for either MLE or MME under both the LN and IG model. This seems to be rather natural, for the same reason that was explained in the previous paragraph. Thus, the obvious conclusion is that the mean of wet durations increases, and the mean of dry durations decreases, as the size of the area increases. Moreover, Table 17 shows that, in all cases, the variance of wet duration increases as the size of the region increases.

Thus, a natural question raised at this point, is whether there is some specific relation between the spatial scale λ and the corresponding mean or variance of wet or dry durations of spatially averaged rain rate.

In the rest of this section, a first attempt is made to investigate the possibility of scaling of the probability distributions of dry and wet epoch durations, with respect to the scale magnification $0<\lambda\leq 1$ applied to the size of a given sub-region $A\subseteq S$ (see Introduction).

Strictly speaking, if W_A denotes the wet epoch duration of spatially averaged rainfall over a sub-region A, of a fixed larger region S, then the stochastic process $\{W_A;\ A\subseteq S\}$, parametrized by the sub-regions $A\subseteq S$, is said to be a self-similar (or simple scaling) process, if and only if there is a fixed constant $\theta \in R$, such that for every $\lambda>0$, the finite dimensional distributions (f.d.d) of the process $\{W_{\lambda A};\ A\subseteq S\}$ coincide with the f.d.d of the process $\{\lambda^{\theta}\cdot W_A;\ A\subseteq S\}$.

If this property holds, then obviously, for every $A\subseteq S$, and for every $\lambda>0$, the random variables $W_{\lambda A}$ and $\lambda^{\theta}\cdot W_A$ will have the same probability distribution, and therefore the same moments, provided that the moments exist.

Thus, simple scaling in the strict sense defined in terms of f.d.d, implies a weaker notion of simple scaling, in the sense that there is a fixed constant $\theta \in R$, such that for every $A \subseteq S$, and for every $\lambda > 0$, it holds that $E\left(W_{\lambda A}^{k}\right) = \lambda^{\theta k} \cdot E\left(W_{A}^{k}\right)$, or equivalently that

$$\log\left\{\frac{M_{\lambda}(k)}{M_{1}(k)}\right\} = \theta \cdot k \cdot \log\lambda \qquad (6),$$

provided that $M_{\lambda}(k) = E\left(W_{\lambda A}^{k}\right) < \infty$, for every $k \geq 1$.

This weaker notion of simple scaling is referred to *as simple-scaling in the wide sense*. For a general discussion or notions of scaling related in particular with rainfall processes, we refer to Kedem and Chiu (1987a), and Gupta and Waymire (1990).

What is actually investigated in this section, is the simple scaling in the wide sense, for the duration of dry and wet epochs.

Note that equation (6) expresses a simple log-log linear relationship between the ratio of k-order moments $M_{\lambda}(k) / M_{1}(k)$, and the scale of magnification $0 < \lambda \leq 1$, whose slope $\theta \cdot k$ is itself a linear function of the moment's order $k \geq 1$. The constant $\theta \in R$ is referred to as *scaling exponent*.

In particular, for k=1 the notation is simplified if we set $M_{\lambda} = M_{\lambda}(1)$ for every $0 < \lambda \leq 1$, and equation (6) reduces to

$$\log\left(\frac{M_{\lambda}}{M_{1}}\right) = \theta \cdot \log\lambda \qquad (7).$$

Also note that if (6) holds true for k=1 and for k=2, then it is elementary to show that also the variances $V_\lambda = V(W_{\lambda A}) = M_\lambda(2) - [M_\lambda(1)]^2$ obey a relation similar to (6) for k=2, namely

$$\log\left(\frac{V_\lambda}{V_1}\right) = 2\theta \cdot \log\lambda \qquad (8).$$

Another elementary consequence of (7) and (8) is that the coefficient of variation $\sqrt{V_\lambda}/M_\lambda$ remains constant for every $0<\lambda\leq 1$, and also that if (7) and (8) hold, then equation (6) for k=2 holds true also.

The exact same arguments may be repeated in order to speak of strict and wide sense simple scaling of the stochastic process $\{D_A;\ A\subseteq S\}$, parametrized by the sub-region $A\subseteq S$, where D_A denotes the dry epoch duration of spatially averaged rainfall over a sub-region A of a fixed region S.

The rest of this section is divided into two sub-sections, where the scaling of dry and wet epoch durations is investigated separately.

5.1 Scaling of Dry Spells

In this subsection it will be shown that there is significant statistical evidence supporting the validity of equations (7) and (8). In other words it will be shown that the mean and the variance of dry epoch durations possess the property of simple scaling. This task will be carried out via simple linear regression of $\log\left(\frac{M_\lambda}{M_1}\right)$ and of $\log\left(\frac{V_\lambda}{V_1}\right)$ on $\log\lambda$, using the MLE and MME estimates of mean and variance of dry durations under the Lognormal (LN) and inverse Gaussian (IG) models.

Table 18 summarizes the MME and MLE estimates of $\log\left(\frac{M_\lambda}{M_1}\right)$ under the LN and IG models. Table 19 summarizes the information of slope, squared correlation, and sum of squared residuals, obtained from the corresponding linear regressions of $\log\left(\frac{M_\lambda}{M_1}\right)$ on $\log\lambda$.

TABLE 18				
LN		IG	Log (λ)	λ
MLE $\log(M_\lambda/M_1)$	MME $\log(M_\lambda/M_1)$	MLE=MME $\log(M_\lambda/M_1)$		
0.4392	0.417	0.417	-1.6094	0.2
0.2536	0.2358	0.236	-0.9163	0.4
0.2314	0.2227	0.223	-0.5108	0.6
0.0846	0.0707	0.071	-0.2231	0.8
0	0	0	0	1

Table 18. The logarithms of the ratios of the means of Dry epoch durations, for scale λ, under the Lognormal and Inverse Gaussian models (MLE and MME), the scale λ and its logarithm.

	TABLE 19		
	Lognormal		Inverse Gaussian
	MLE	MME	MLE=MME
Squared Corr.	0.97417	0.97280	0.97274
Slope	-0.287698	-0.271809	-0.271832
SSR	0.00820883	0.00772644	0.00774697

Table 19. Squared correlation, Slope, and Sum of Squared Residuals of regressions of $\log(M_\lambda/M_1)$ on $\log\lambda$ under LN and IG models for dry durations.

Figure 1 shows the plots of the points ($\log\lambda$, $\log(M_\lambda/M_1)$), and of the best fitting straight line obtained from the corresponding linear regression.

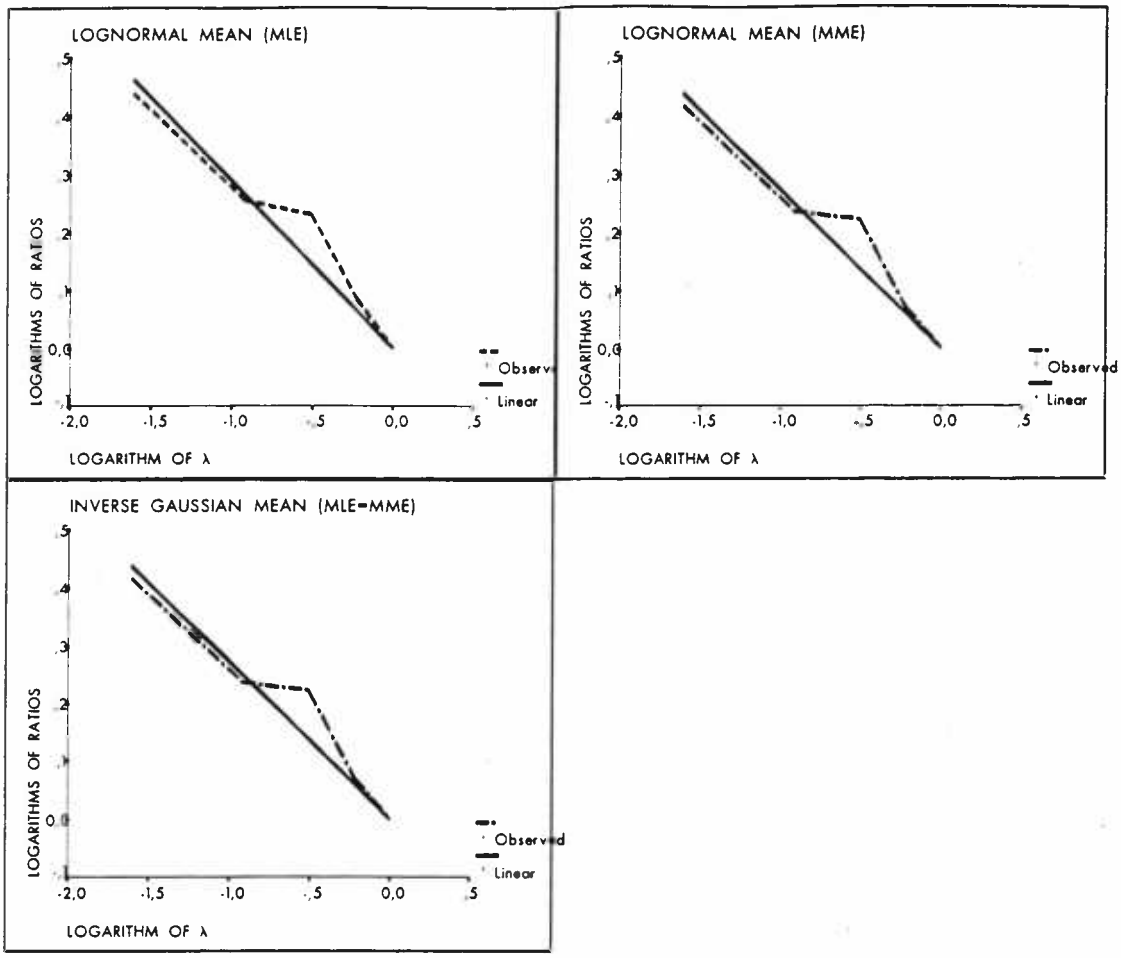

Figure 1. Regressions of $\log(M_\lambda/M_1)$ on $\log\lambda$ under LN and IG model for dry durations.

It is clear that, under both models (LN and IG), the squared correlation is quite high, the sums of squared residuals extremely low, and the negative slope values quite close to one another.

Table 20 summarizes the MME and MLE estimates of $\log(V_\lambda/V_1)$ under the LN and IG models. Table 21 summarizes the information of slope, squared correlation, and sum of squared residuals, obtained from the corresponding linear regression of $\log(V_\lambda/V_1)$ on $\log\lambda$.

TABLE 20					
LN		IG		Log (λ)	λ
MLE $\log(V_\lambda/V_1)$	MME $\log(V_\lambda/V_1)$	MLE $\log(V_\lambda/V_1)$	MME $\log(V_\lambda/V_1)$		
1.291276	1.09165	1.1931125	1.091561	-1.60944	0.2
0.797473	0.499954	0.7047426	0.500007	-0.91629	0.4
0.64194	0.45852	0.5986597	0.458811	-0.51083	0.6
0.151645	0.061012	0.1264889	0.060963	-0.22314	0.8
0	0	0	0	0	1

Table 20. The logarithms of the ratios of the variances of Dry epoch durations, for scale λ, under the Lognormal and Inverse Gaussian models (MLE and MME), the scale λ and its logarithm.

	TABLE 21			
	Lognormal		Inverse Gaussian	
	MLE	MME	MLE	MME
Squared Corr.	0.98145	0.97946	0.97984	0.97942
Slope	-0.847650	-0.658415	-0.775270	-0.658444
SSR	0.0508001	0.0340119	0.0462552	0.0340686

Table 21. Squared correlation, Slope, and Sum of Squared Residuals of regressions of $\log(V_\lambda/V_1)$ on logλ under LN and IG models for dry durations.

Figure 2 shows the plots of the points (logλ, $\log(V_\lambda/V_1)$), and of the best fitting straight line obtained from the corresponding linear regression.

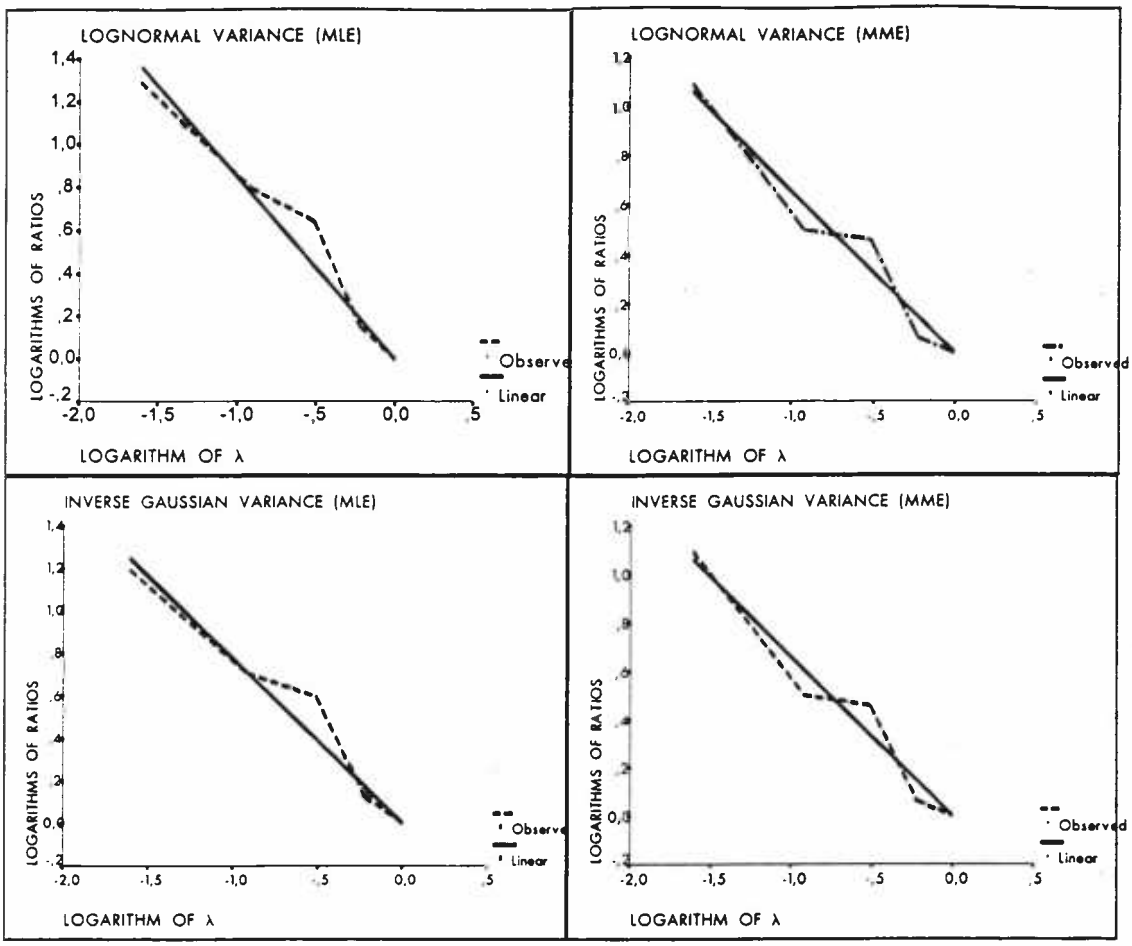

Figure 2. Regressions of $\log\left(V_\lambda / V_1\right)$ on $\log\lambda$ under LN and IG model for dry durations.

Again, these fits are quite remarkable under both LN and IG models. Also note that if $\hat{\theta}_{dry} = -0.2718$ is used as an estimate of the scaling exponent for the mean (Table 19), then $2\hat{\theta}_{dry} = -0.5436$ is not really very close to the estimated values of the slope of (8) (Table 21). This deviation may be due to some partial inadequacy of the assumed parametric models.

Thus, under the adoption of either one of the LN or IG models, the first two moments of dry epoch duration seem to conform with the property of wide sense simple scaling.

However, if one is not willing to adopt a specific parametric model (such as IG or LN) for the probability distribution of dry epoch duration, then one should simply rely on the non-parametric sample estimates of the moments

$$\hat{M}_{\lambda}(k) = \frac{1}{N}\sum_{n=1}^{N}\phi_n^k(\lambda),$$

and to proceed with the linear regressions of $\log\left[\hat{M}_{\lambda}(k)/\hat{M}_{1}(k)\right]$ on $\log\lambda$ in order to test the validity of equation (6) for each $k\geq 1$. This task has indeed been carried out for the first twenty moments ($1\leq k\leq 20$) of dry epoch durations, and the information of the corresponding linear regression is summarized in Table 22.

TABLE 22. DRY SAMPLE MOMENTS AND REGRESSION INFORMATION

ORD	$\hat{M}_{0.2}(k)$	$\hat{M}_{0.4}(k)$	$\hat{M}_{0.6}(k)$	$\hat{M}_{0.8}(k)$	$\hat{M}_{1}(k)$	SLOPE	R SQRD	SSR
1	2.16	1.8	1.78	1.53	1.42	-0.273868	0.97149	0.00823342
2	16.03	9.54	9.2	6.39	5.84	-0.622095	0.98141	0.0274201
3	216.66	73.24	69.77	40.72	38.45	-0.986545	0.96751	0.1222541
4	4031.1	648.37	612.45	310.81	317.9	-1.355674	0.93023	0.5156458
5	88679.46	6171.93	5791.77	2606.71	2997.37	-1.715966	0.88478	1.43441
6	2113974.3	61505.76	57418.23	23174.74	30753.33	-2.058314	0.84091	2.998245
7	52267698	633421.42	589024.44	214570.13	334114.76	-2.38165	0.802	5.23822
8	1314000000	6690335.9	6205551.3	2048011.8	3776025.5	-2.689407	0.76871	8.140436
9	33270000000	72099112	66797263	20018185	43854810	-2.985742	0.74076	11.670046
10	8.455E+11	789702759	731782552	199428072	518992914	-3.274805	0.71755	15.791044
11	2.152208E+13	8764991838	8133997313	2017661243	6221752583	-3.5595	0.69839	20.46715
12	5.483258E+14	98346428610	91500674379	20671372221	75250434672	-3.8418	0.68263	25.66851
13	1.39758E+16	1113446466622	1039533316764	213967292563	915674580583	-4.1233	0.66966	31.37046
14	3.56295E+17	1.270079E+13	1.190704E+13	2233396492191	1.118876E+13	-4.4046	0.65898	37.55404
15	9.084319E+18	1.457876E+14	1.373134E+14	2.347235E+13	1.37109E+14	-4.6864	0.65015	44.20495
16	2.316335E+20	1.68236E+15	1.592466E+15	2.480694E+14	1.683475E+15	-4.9689	0.64283	51.31259
17	5.906424E+21	1.950235E+16	1.855543E+16	2.633713E+15	2.069849E+16	-5.2522	0.63673	58.86926
18	1.506106E+23	2.269596E+17	2.170633E+17	2.806577E+16	2.547299E+17	-5.5365	0.63163	66.86942
19	3.840525E+24	2.650191E+18	2.547692E+18	2.999859E+17	3.136931E+18	-5.8216	0.627334	75.30915
20	9.793276E+25	3.103738E+19	2.998696E+19	3.214378E+18	3.864804E+19	-6.1076	0.6237	84.18573

Table 22. Tabulation of Dry sample moments of order $k=1,\ldots,20$ and the results (slope, R squared, and Sum of Squared Residuals) of regressions of $\log\left[\hat{M}_{\lambda}(k)/\hat{M}_{1}(k)\right]$ on $\log\lambda$.

Clearly enough, for k≥5 the squared correlation between $\log\left[\hat{M}_\lambda(k)/\hat{M}_1(k)\right]$ and $\log\lambda$ becomes rather poor to support the validity of equation (6) beyond the fourth moment.

However, the pseudo-slopes A(k) are highly correlated with the corresponding moment's order k, with squared correlation coefficient 0.999, and sum of squared residuals 0.2673. The best fitting line through the origin to the points (k, A(k)), estimated on the basis of $1\le k\le 20$, is given by the equation $A(k) = -0.3138\cdot k$. That is, the pseudo-scaling exponent of dry durations is estimated by $\hat{\theta}_{dry} = -0.3138$.

5.2 Scaling of Wet Spells

Work similar to that presented in the previous subsection, is done here in order to investigate the scaling properties of wet epoch durations.

Table 23 summarizes the MME and MLE estimates of $\log(M_\lambda/M_1)$, under the LN and IG models for the duration of wet epochs. Table 24 summarizes the information of slope, squared correlation, and sum of squared residuals, obtained from the corresponding linear regressions of $\log(M_\lambda/M_1)$ on $\log\lambda$.

TABLE 23				
LN		IG	Log (λ)	λ
MLE $\log(M_\lambda/M_1)$	MME $\log(M_\lambda/M_1)$	MLE=MME $\log(M_\lambda/M_1)$		
-0.324	-0.3174	-0.3174	-1.6094	0.2
-0.2235	-0.2239	-0.2238	-0.9163	0.4
-0.0205	-0.05855	-0.0585	-0.5108	0.6
-0.0467	-0.0416	-0.0415	-0.2231	0.8
0	0	0	0	1

Table 23. Tabulation of the logarithms of the ratios of the means of Wet epoch durations, for scale λ, under the Lognormal and Inverse Gaussian models (MLE and MME), the scale λ and its logarithm.

	TABLE 24		
	Lognormal		Inverse Gaussian
	MLE	MME	MLE=MME
Squared Corr.	0.94734	0.97713	0.97713
Slope	0.199742	0.201892	0.201855
SSR	0.00829619	0.00356924	0.00356662

Table 24. Squared correlation, Slope, and Sum of Squared Residuals of regressions of $\log(M_\lambda/M_1)$ on $\log\lambda$ under LN and IG models for wet durations.

Figure 3 shows the plots of the points ($\log\lambda$, $\log(M_\lambda/M_1)$), and of the best fitting straight line obtained from the corresponding linear regression.

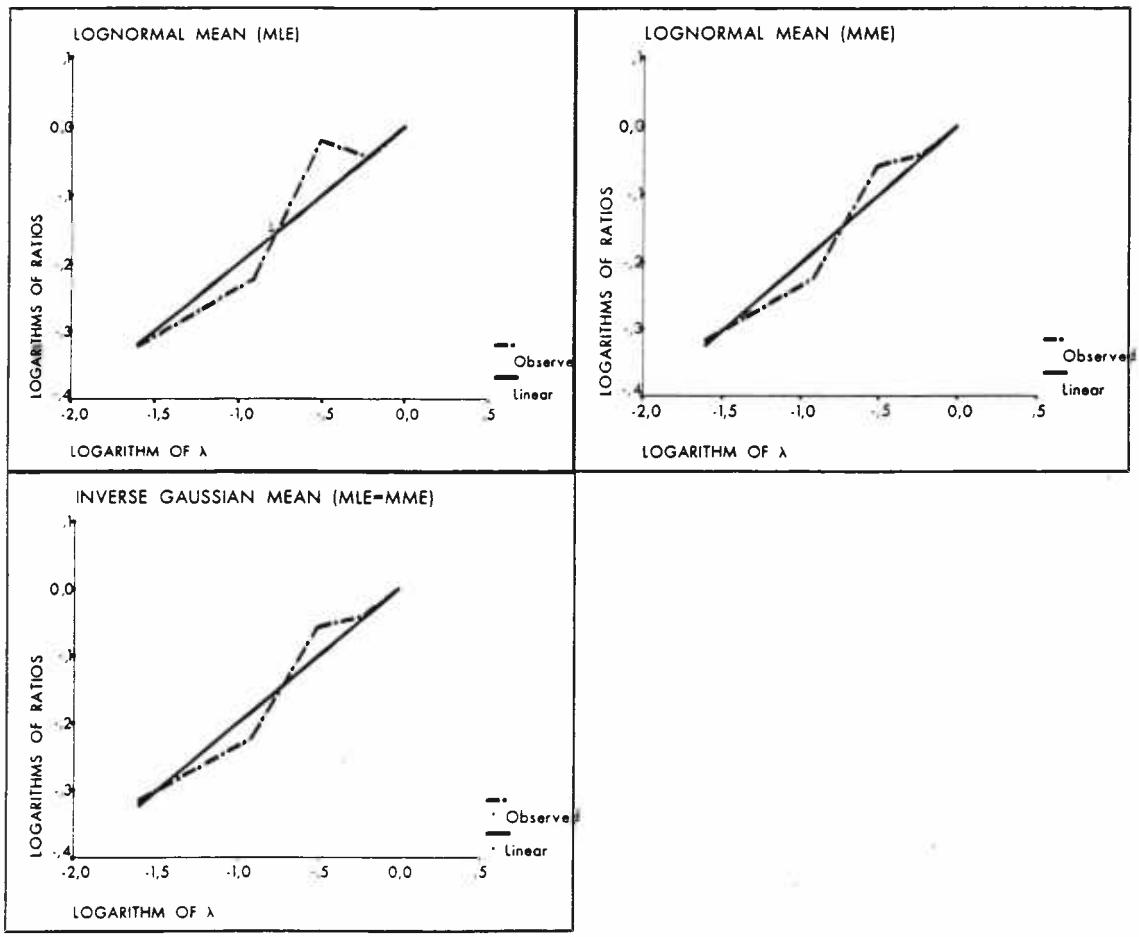

Figure 3. Regressions of $\log(M_\lambda/M_1)$ on $\log\lambda$ under LN and IG model for wet durations.

All the same, under both LN and IG models, the squared correlation is remarkably high (MME cases), the sums of squared residuals extremely low, and the positive slope values quite close to one another.

Table 25 summarizes the MME and MLE estimates of $\log(V_\lambda/V_1)$, under the LN and IG models for the duration of wet epoch durations. Table 26 summarizes the information of slope, squared correlation, and sums of squared residuals, obtained from the corresponding linear regressions of $\log(V_\lambda/V_1)$ on $\log\lambda$.

TABLE 25					
LN		IG		Log (λ)	λ
MLE $\log(V_\lambda/V_1)$	MME $\log(V_\lambda/V_1)$	MLE $\log(V_\lambda/V_1)$	MME $\log(V_\lambda/V_1)$		
-0.9807	-0.8071	-0.9354	-0.8071	-1.6094	0.2
-0.7738	-0.5814	-0.7339	-0.5812	-0.91629	0.4
-0.2107	-0.3904	-0.2933	-0.3902	-0.5108	0.6
-0.185	-0.0862	-0.1566	-0.0859	-0.22314	0.8
0	0	0	0	0	1

Table 25. Tabulation of the logarithms of the ratios of the variances of Wet epoch durations, for scale λ, under the Lognormal and Inverse Gaussian models (MLE and MME), the scale λ and its logarithm.

	TABLE 26			
	Lognormal		Inverse Gaussian	
	MLE	MME	MLE	MME
Squared Corr.	0.96806	0.97790	0.97916	0.97794
Slope	0.651314	0.548137	0.631635	0.548043
SSR	0.0523535	0.0253949	0.0317645	0.0253409

Table 26. Squared correlation, Slope, and Sum of Squared Residuals of regressions of $\log(V_\lambda/V_1)$ on $\log\lambda$ under LN and IG models for wet durations.

Figure 4 shows the plots of the points $(\log\lambda,\ \log(V_\lambda/V_1))$, and of the best fitting straight line obtained from the corresponding linear regression.

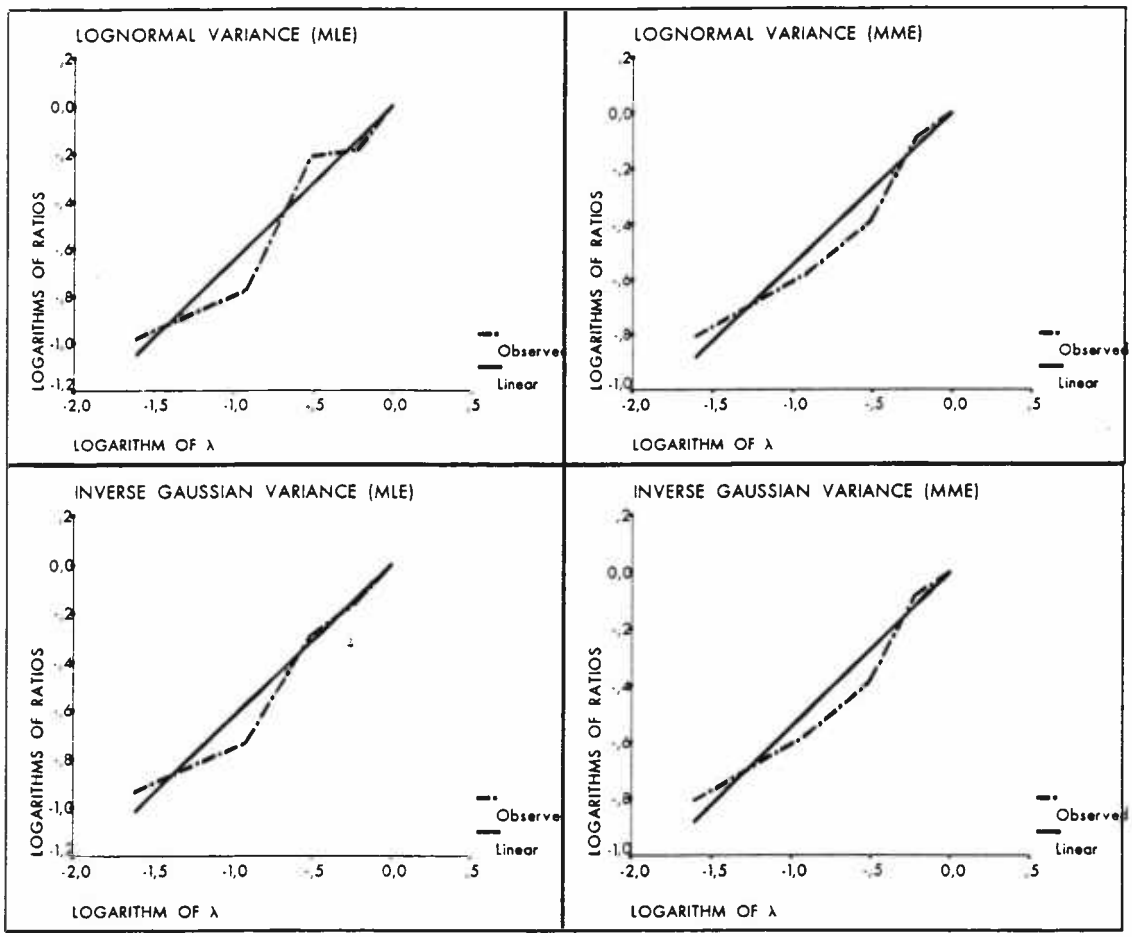

Figure 4. Regressions of $\log(V_\lambda/V_1)$ on $\log\lambda$ under LN and IG model for wet durations.

Again, under both LN and IG models, the squared correlation is remarkably high, and the sums of squared residuals low enough. Also note that if $\hat{\theta}_{wet} = 0.2018$ is used as an estimate of the scaling exponent for the mean of wet durations (Table 24), then $2\hat{\theta}_{wet} = 0.4036$ is not very close to the estimated values of the slope of (8) (Table 26). This discrepancy may again be attributed to some partial inadequacy of LN and IG in modeling the distribution of wet epoch durations.

Therefore, under the adoption of either one of the LN or IG models, there is rather significant indication that the first two moments of wet epoch durations do conform with the property of wide sense simple scaling. This indication is supported by the very significant correlation in the log-log linear relations (7) and (8), but it is slightly shattered by the non-exact doubling rule between the estimates of the corresponding slopes θ and 2θ of (7) and (8).

Thus, it is of interest to resort to non-parametric sample estimates of the moments

$$\hat{M}_{\lambda}(k) = \frac{1}{N}\sum_{n=1}^{N} \psi_n^k(\lambda)$$

of Wet epoch durations (for $0 < \lambda \leq 1$), and to proceed with the linear regressions of $\log\left[\hat{M}_{\lambda}(k)/\hat{M}_{1}(k)\right]$ on $\log\lambda$, for $k \geq 1$, in order to verify or reject the hypothesis of wide sense simple scaling of wet epoch durations.

This task has indeed been carried out for the first twenty sample moments ($1 \leq k \leq 20$) of wet epoch durations, and the information of the corresponding linear regressions is summarized in Table 27.

Figure 5 depicts the plots of the points ($\log\lambda$, $\log\left(\hat{M}_{\lambda}(k)/\hat{M}_{1}(k)\right)$), and the best fitting straight line obtained from the corresponding linear regression, only for a small selection of values of k=1, 2, 10, 20. Quite similar are also the graphs corresponding to the rest of the values of k.

TABLE 27. WET SAMPLE MOMENTS AND REGRESSION INFORMATION								
ORD	$\hat{M}_{0.2}(k)$	$\hat{M}_{0.4}(k)$	$\hat{M}_{0.6}(k)$	$\hat{M}_{0.8}(k)$	$\hat{M}_{1}(k)$	SLOPE	R SQRD	SSR
1	0.76	0.84	0.99	1	1.05	0.204678	0.97873	0.00340497
2	1.59	1.97	2.51	3.09	3.36	0.497537	0.98826	0.01099755
3	5.6	8.33	10.62	16.55	18.28	0.78163	0.98416	0.0367802
4	25.22	46.83	58.41	112.02	123.73	1.030742	0.98204	0.0726831
5	129.35	302.74	368.53	847.07	932.16	1.257678	0.9803	0.1189061
6	712.89	2099.42	2501.41	6804.51	7473.83	1.477147	0.97854	0.1789546
7	4096.61	15121.1	17685.2	56771.48	62465.49	1.697726	0.97691	0.254829
8	24154.69	111388.43	128168.45	486168.44	537979.46	1.922936	0.97552	0.347029
9	144849.3	832720.05	944293.2	4243094.2	4738702.2	2.153481	0.97441	0.45555
10	878890.52	6290558.2	7040505.1	37563632	42460773	2.388861	0.97354	0.580112
11	5378685.3	47891135	52974736	336192929	385483413	2.628164	0.97287	0.720383
12	33131109	366786240	401508660	3.034E+09	3.535E+09	2.870483	0.97237	0.875801
13	205111156	2.822E+09	3.061E+09	2.757E+10	3.267E+10	3.115072	0.97198	1.046443
14	1.275E+09	2.18E+10	2.345E+10	2.518E+11	3.037E+11	3.361042	0.97167	1.231871
15	7.95E+09	1.688E+11	1.804E+11	2.309E+12	2.836E+12	3.608249	0.97146	1.430712
16	4.971E+10	1.31E+12	1.392E+12	2.124E+13	2.658E+13	3.85628	0.9713	1.643822
17	3.115E+11	1.019E+13	1.077E+13	1.96E+14	2.498E+14	4.104643	0.97115	1.872087
18	1.955E+12	7.938E+13	8.357E+13	1.812E+15	2.353E+15	4.353466	0.97107	2.112417
19	1.229E+13	6.189E+14	6.494E+14	1.678E+16	2.22E+16	4.602478	0.971	2.366864
20	7.735E+13	4.831E+15	5.053E+15	1.556E+17	2.098E+17	4.851893	0.97094	2.635609

Table 27. Tabulation of Wet sample moments of order k=1,...,20 and the results (slope, R squared, and Sum of Squared Residuals) of regressions of $\log\left[\hat{M}_{\lambda}(k)/\hat{M}_{1}(k)\right]$ on $\log\lambda$.

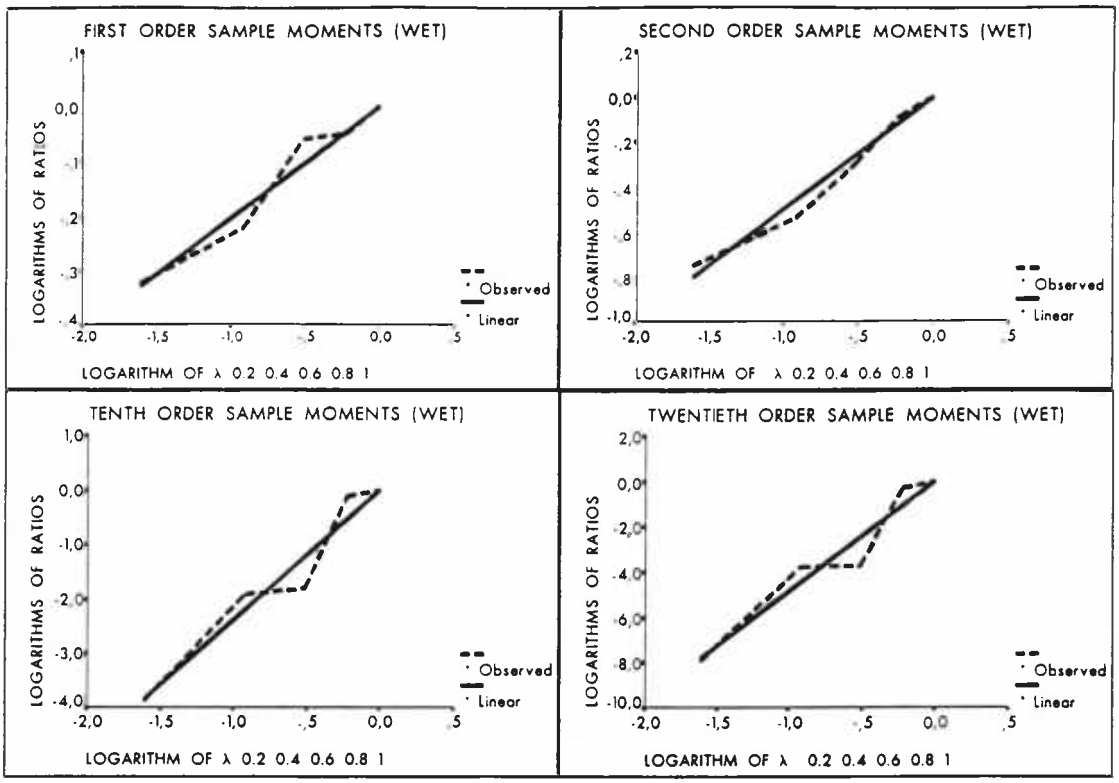

Figure 5. Regressions of $\log\left[\hat{M}_\lambda(k)/\hat{M}_1(k)\right]$ on $\log\lambda$ for order $k=1, 2, 10, 20$ of wet sample moments.

Remarkable enough is the fact that the values of the squared correlation in Table 27, are persistently very high, between 97% up to almost 99%, throughout the range of $1\le k\le 20$. This is indeed a strong piece of evidence supporting the log-log linear relationship between the ratio $M_\lambda(k)/M_1(k)$ of moments of wet epoch durations and the parameter of spatial scale λ, for every $1\le k\le 20$, as required according to equation (6).

On the other hand, the sums of squared residuals are growing as the order k increases. This growth is slower for the first ten orders, compared to the growth corresponding to larger orders k, and also more conducive to the goodness of fit of the best fitting straight line.

However, more striking of all is the perfectly linear growth of the slope of the corresponding best fitting straight line, as the order k increases. This perfection is easily detectable even by eye, if the slope A(k) is plotted against the order k as in Figure 6.

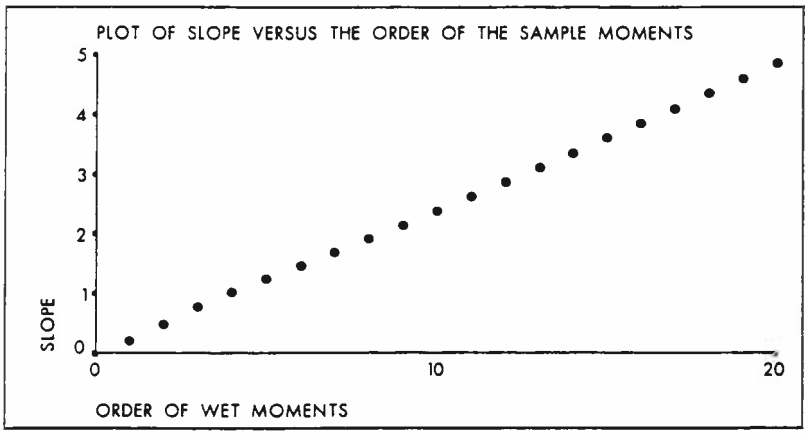

Figure 6. Plot of the slope A(k) versus the order k=1,..., 20 of wet sample moments.

Obviously, the slope of the best fitting straight line, passing through the origin (0, 0) to the points with coordinates (k, A(k)) of Figure 6, will provide an estimate of the scaling exponent $\theta_{wet} > 0$. Indeed, linear regression of the slopes A(k) on k, yields squared correlation coefficient 0.9999, sum of squared residuals 0.01703, and the corresponding equation of the best fitting line through the origin is $A(k) = 0.2414 \cdot k$. Therefore, $\hat{\theta}_{wet} = 0.2414$ is the estimated value of the scaling exponent of wet epoch duration with respect to the spatial scale of the region over which rain rate is spatially averaged.

CHAPTER 6

CONCLUSION

On the basis of some literature and empiricism, the parametric families of lognormal, of Inverse Gaussian, and of Gamma distributions have been proposed as plausible models for the probability distribution of dry and of wet epoch duration in processes of spatially averaged (instantaneous) rain rate.

Real data of such dry and wet epoch durations, obtained from the TOGA-COARE measurements of tropical rainfall on an array of nested square regions, whose sizes vary from 10×10 km^2 to 2×2 km^2, have been used for testing the goodness of fit of the proposed distribution models. The fits of the gamma model are very poor in all spatial scales, indicating the inadequacy of the model. The fits of both the lognormal and the Inverse Gaussian models are very good in all spatial scales, for both dry and wet epoch durations. Nevertheless, in all cases the fit of Inverse Gaussian is considerably better than the corresponding fit under the lognormal model.

This fact is also supported on a theoretical basis, since according to the model proposed by Freidlin and Pavlopoulos (1997), it follows that the probability distribution of dry and wet epoch durations, in a given atmospheric column, belongs to the Inverse Gaussian family and its parameters are physically interpretable. On the other hand, the plausibility of the lognormal model is based mostly on empiricism, and the only available theoretical explanation is of heuristic nature (Biondini (1976), Lopez (1977)).

In the sequel, under the assumption that the probability distributions of dry and of wet epoch duration are of continuous type (i.e. without discrete atoms), the Wald-Wolfowitz test for runs above and below the median has been employed in order to test the hypothesis of randomness (that is, i.i.d. structure) in data of dry and wet epoch durations.

The results of this non-parametric test show that in all spatial scales the hypothesis of randomness in data of wet epoch duration is not rejected for levels of significance $\alpha \leq 0.15$, since the obtained p-values are all higher than 15% (see Table 3). This fact provides enough evidence supporting the hypothesis of randomness in data of wet epoch duration. On the other hand, the hypothesis of randomness in data of dry epoch duration is not rejected for levels of significance $\alpha \leq 0.26$ in areas of size 6×6 km^2 or larger, and it is not rejected for levels $\alpha \leq 0.02$ in areas of smaller size (see Table 2). Thus, one may argue that as the size of the region decreases, the randomness of dry durations tends to be rejectable for levels of significance higher than 2%. Nevertheless, at the strict level of significance $\alpha = 0.01$, TOGA-COARE data support the hypothesis of randomness, both of dry and of wet durations of spatially averaged rain rate, for all spatial scales. This conclusion is also in agreement with the theoretically implied randomness of dry and wet epoch durations, according to the model introduced by Freidlin and Pavlopoulos (1997).

The last part of this dissertation has been concerned with the dependence of the probability distribution, and more specifically of the moments, of wet and dry duration, on the scale λ of the region over which rain rate is (spatially) averaged. Under both models, lognormal and Inverse Gaussian, it has been shown that the mean and the variance of dry and of wet duration, are (simply) scaling in the sense

of equations (7) and (8) respectively. From these first indications, one may conceivably attribute the scaling to strict self similarity of the processes $\{D_A ; A \subseteq S\}$ and $\{W_A ; A \subseteq S\}$, of dry and wet epoch duration respectively. However, if this was indeed true, then there should be two scaling exponents θ_{dry} and θ_{wet}, such that in the sense of finite dimensional distributions the equalities $\{D_{\lambda A} ; A \subseteq S\} = \{\lambda^{\theta_{dry}} \cdot D_A ; A \subseteq S\}$ and $\{W_{\lambda A} ; A \subseteq S\} = \{\lambda^{\theta_{wet}} \cdot W_A ; A \subseteq S\}$ should hold, for every $\lambda > 0$. Consequently, the slope of the log-log linear relationship between the ratio of the variances V_λ / V_1 and the spatial scale λ, should equal twice the slope of the log-log linear relationship between the ratio of means M_λ / M_1 and λ.

In fact though, the obtained estimates of these slopes, for dry and wet durations, under lognormal or Inverse Gaussian model, revealed a deviation from this "doubling rule". This masking of the "doubling rule" has been attributed to potential imperfections of both the lognormal and the Inverse Gaussian models.

Thus, the investigation, of simple scaling of the moments of dry and wet duration, in the sense of the log-log linear relationship (6), with linear slope $A(k) = \theta \cdot k$, has been based on the non-parametric sample estimates of the moments $\hat{M}_\lambda(k)$, where k denotes the order of the moment and λ is the spatial scale. Working with moments of order $1 \le k \le 20$, and values of spatial scale λ =1, 0.8, 0.6, 0.4, 0.2, Tables 22 and 27 show the extremely rapid growth of moments as the order k increases, both for dry and wet durations respectively.

In the case of dry durations, simple scaling of the sample moments does not seem to hold, since the squared correlation between $\log(\hat{M}_\lambda(k)/\hat{M}_1(k))$ and $\log\lambda$

drops significantly for values of the order $k \geq 5$. Therefore, the process $\{D_A ; A \subseteq S\}$ is rather unlikely to possess the property of self-similarity.

In the case of wet durations, there is indeed strong evidence of simple scaling of the sample moments, since the squared correlation between $\log(\hat{M}_\lambda(k)/\hat{M}_1(k))$ and $\log\lambda$ maintains remarkably high values, greater than 0.97, for every $1 \leq k \leq 20$, so as to support the validity of the log-log linear relationship $\log(M_\lambda(k)/M_1(k)) = A(k) \cdot \log\lambda$. Moreover, the slope A(k) is a linear function of the order k, with slope estimated by $\hat{\theta}_{wet} = 0.2414$. Therefore, the process $\{W_A ; A \subseteq S\}$ is likely to be a self-similar process with respect to the spatial scale $0 < \lambda \leq 1$, and if this is truly the case, then $\hat{\theta}_{wet} = 0.2414$ is an estimate of the corresponding scaling exponent.

The practical value of self-similarity of the process $\{W_A ; A \subseteq S\}$ of wet epoch duration of spatially averaged rain rate, parametrized by the subregions A of a larger region of interest S, is the fact that it makes possible the drawing of inferences about the duration of rainfall in the region S on the basis of data of rainfall duration in smaller subregions of S. That is, if S is associated with the spatial scale of reference $\lambda = 1$, then any other subregion $A \subseteq S$ may be associated with a spatial scale value $0 < \lambda \leq 1$, and in light of self similarity the probability distribution of W_S coincides with the probability distribution of $\lambda^{-\theta_{wet}} \cdot W_A$. Thus, knowing the distribution or the moments of $W_A = W_{\lambda S}$, and having an estimate of the scaling exponent θ_{wet}, it is possible to make inferences about the duration of rainfall W_S on the larger region S. This application is of great interest with regard to large tropical

and sub-tropical regions where networks of monitoring stations are very limited due to physical constraints, such as oceanic surface or rainforest jungle.

REFERENCES

Aitchison, J. and J.A.C. Brown (1963). ***The Lognormal Distribution***, Cambridge Univ. Press.

Bhattacharya, R.N. and E.C. Waymire (1990). ***Stochastic Processes with Applications***, Wiley.

Biondini, R. (1976). Cloud Motion and Rainfall Statistics, ***Journal of Applied Meteorology***, 15, 205-224.

Brownlee, K.A. (1965). ***Statistical Theory and Methodology in Science and Engineering***, Second Edition, J.Wiley & Sons.

Cramer, H. (1974). ***Mathematical Methods of Statistics***, Princeton University Press.

Crovelli, R.A. (1971). ***Stochastic Models for Precipitation***, Ph.D. Dissertation, Dept. of Statistics, Colorado State University, Fort Collins.

Crow, E.L. and K. Shimizu (1988). ***Lognormal Distributions***, Marcel Dekker.

Eagleson, P. (1978). Climate, Soil, and Vegetation 2, The Distribution of Annual Precipitation Derived from Observed Storm Sequences, ***Water Resources Research***, 14, 713-721.

Freidlin, M. and H. Pavlopoulos (1997). On a Stochastic Model for Moisture Budget in an Eulerian Atmospheric Column, ***Environmetrics*** (To Appear).

Grayman, W.M. and P. Eagleson (1971). ***Evaluation of Radar and Raingage Systems for Flood Forecasting***, R.M.P Lab. Report 138, Mass. Inst. of Technology, Cambridge, Massachusetts.

Gupta, V. and E.C. Waymire (1990). Multiscaling properties of spatial rainfall and river flow distributions, ***Journal of Geophysical Research***, 95, 1999-2009.

Gupta, V.K. and E.C. Waymire (1993). A Statistical Analysis of Mesoscale Rainfall as a Random Cascade, ***Journal of Applied Meteorology***, 32, 251-267.

Houze, R.A. and C.C. Cheng (1977). Radar Characteristics of Tropical Convection Observed During GATE: Mean Properties and Trends Over the Summer Season, ***Monthly Weather Review***, 105, 964-980.

Johnson, N.L. and S. Kotz (1970). ***Continuous Univariate Distributions-I***, J.Wiley & Sons.

Karlin, S. and H.M. Taylor (1975). ***A First Course in Stochastic Processes***, 2nd Edition, Academic Press.

Kedem, B. and L.S. Chiu (1987a). Are Rain Rate Processes Self Similar?, ***Water Resources Research***, 23, 1816-1818.

Kedem, B. and L.S. Chiu (1987b). On the Lognormality of Rain Rate, ***Proceedings of the National Academy of Sciences***, USA, 84, 901-905.

Kedem, B., L.S. Chiu, and G.R. North (1990). Estimation of Mean Rain Rate: Application to Satellite Observations, ***Journal of Geophysical Research***, 95, 1965-1972.

Kedem, B., R. Pfeiffer, and D. Short (1997). Variability of Space-Time Mean Rain Rate, ***Journal of Applied Meteorology***, 36, 443-551.

LeCam, L. (1961). ***A Stochastic Description of Precipitation***, Fourth Berkeley Symposium on Statistics and Probability, Univ. of California, Berkeley, California.

Lopez, R.E. (1977). The Lognormal Distribution and Cumulus Cloud Populations, ***Monthly Weather Review***, 105, 865-872.

Pavlopoulos, H. and B. Kedem (1992). Stochastic Modeling of Rain Rate Processes: A Diffusion Model, ***Stochastic Models***, 8, 397-420.

Peters, W. and G. Summers (1968). ***Statistical Analysis for Business Decisions***, Prentice-Hall.

Short, D., K. Shimizu, and B. Kedem (1993). Optimal Thresholds for the Estimation of Area Rain-Rate Moments by the Threshold Method, ***Journal of Applied Meteorology***, 32, 182-192.

Wallis, W.A. (1952). Rough-and-Ready Statistical Tests, ***Industrial Quality Control***, V. 8, 35-40.

Waymire, E.C. and V. Gupta (1981a). The Mathematical Structure of Rainfall Representations: A Review of the Stochastic Rainfall Models, ***Water Resources Research***, 17, 1261-1272.

Waymire, E.C. and V. Gupta (1981b). The Mathematical Structure of Rainfall Representations: A Review of the Theory of Point Processes, ***Water Resources Research***, 17, 1273-1285.

Waymire, E.C. and V. Gupta (1981c). The Mathematical Structure of Rainfall Representations: Some Applications of the Point Process Theory to Rainfall Processes, ***Water Resources Research***, 17, 1287-1294.

Wolfowitz, J. (1944). Asymptotic Distribution of Runs Up and Down, ***Annals of Mathematical Statistics***, V. 15, 163-172.

Yamane, T. (1973). ***Statistics, An Introductory Analysis (Third Edition)***, Harper.

APPENDIX.

The Appendix includes the following ten tables (Tables A-J) which contain the Dry and Wet blocks converted to units of hours. They correspond to five different sizes of examined areas of the TOGA-COARE experiment.

TABLE A			
2.5	0.3333	0.1667	1.5
1	0.3333	5.5	0.1667
4.5	0.6667	3.1667	5
0.5	0.1667	1.3333	0.3333
0.5	0.1667	0.5	2.8333
1	0.5	0.3333	3
2	0.6667	1.5	2.5
1.8333	3.3333	0.3333	4.1667
0.6667	0.3333	0.1667	2.1667
0.6667	0.1667	0.1667	1.3333
0.3333	1.8333	0.1667	10.8333
3.5	0.1667	0.1667	0.1667
0.6667	7.5	0.1667	0.8333
0.6667	0.1667	10.8333	0.6667
0.1667	0.1667	1	0.1667
1.1667	4.1667	0.3333	4.5
0.3333	11	0.3333	3
0.1667	1.5	4	8.8333
0.8333	0.3333	14.1667	
0.1667	0.5	9.1667	
0.5	0.1667	3.6667	
0.1667	1.6667	9.5	
0.3333	8.3333	0.6667	
3.1667	1.3333	4.8333	
4	1	2.3333	
3	0.1667	5	
2	1.5	1.6667	
0.1667	0.3333	0.1667	
0.5	0.3333	2.5	
25.5	0.1667	1.6667	
0.1667	0.1667	1.1667	
0.1667	7.6667	1.5	
2.5	1.6667	0.1667	
0.6667	0.3333	0.1667	
0.1667	2.3333	0.8333	
1.1667	1.3333	1.5	
0.1667	0.8333	7.3333	
0.1667	1.3333	0.8333	
0.8333	0.3333	0.8333	
0.1667	2.3333	9.8333	

Table A. Lengths of the dry blocks of rain rate averages converted to units of hours over a 2×2 km^2 region of TOGA-COARE in sequence by column.

TABLE B			
0.1667	5.3333	3.5	1.6667
0.1667	0.6667	2	0.1667
0.1667	0.1667	0.1667	0.3333
0.5	0.1667	0.1667	0.3333
6.3333	2	0.8333	0.6667
1.5	4.5	0.1667	1.5
0.1667	1	0.1667	1.3333
0.1667	0.3333	0.3333	0.3333
0.3333	0.1667	0.1667	0.5
1.6667	0.3333	2.1667	0.5
0.8333	0.6667	2.5	0.3333
0.8333	0.1667	0.1667	0.6667
0.8333	0.1667	2.8333	0.1667
0.3333	0.1667	0.1667	0.5
0.1667	0.1667	2.8333	0.1667
0.1667	2	2.5	0.1667
0.1667	0.8333	0.1667	0.1667
0.3333	0.3333	0.3333	0.3333
0.5	0.1667	0.1667	1
2	0.5	1	0.1667
0.5	0.3333	0.1667	0.1667
0.1667	0.1667	0.1667	0.1667
0.3333	0.1667	0.6667	0.3333
0.1667	0.3333	0.1667	0.5
1.3333	0.6667	0.1667	
0.3333	0.3333	1.8333	
0.8333	0.1667	0.8333	
1.1667	0.3333	3.3333	
3.3333	0.1667	0.3333	
0.1667	0.1667	0.6667	
0.3333	0.1667	0.6667	
0.5	2.1667	0.1667	
0.3333	0.1667	0.1667	
0.1667	0.1667	1	
0.1667	0.3333	0.1667	
1.1667	0.3333	0.1667	
1	0.1667	2	
1.3333	0.5	0.1667	
0.8333	0.1667	0.1667	
1.1667	1.8333	1	

Table B. Lengths of the wet blocks of rain rate averages converted to units of hours over a 2×2 km^2 region of TOGA-COARE in sequence by column.

TABLE C			
1.3333	0.1667	0.3333	1.1667
0.8333	0.5	0.1667	1.5
1	0.1667	2	0.1667
4.5	0.3333	0.1667	0.3333
0.5	0.3333	5.5	1.5
0.3333	0.6667	3.1667	7.3333
1	0.3333	0.5	0.6667
2	0.3333	0.3333	0.8333
0.1667	3.3333	0.5	9
0.6667	0.1667	0.3333	0.3333
0.1667	0.1667	1.5	1.5
0.6667	0.8333	0.1667	0.1667
0.1667	0.8333	0.1667	4.8333
3.1667	0.1667	0.1667	0.1667
0.1667	7.3333	0.1667	0.1667
0.1667	0.1667	1	2.3333
0.3333	3.8333	2	2.6667
0.1667	10.833	7.1667	1.6667
1.1667	1.3333	0.6667	0.5
0.5	0.1667	0.1667	3.8333
0.5	0.1667	0.3333	0.3333
0.1667	0.1667	0.1667	1.1667
0.1667	1	0.1667	1
3.1667	0.5	0.3333	9.3333
0.6667	8	2.6667	1
3.1667	0.1667	6.3333	0.1667
2.8333	1	7.5	0.3333
2	0.5	9	0.5
0.1667	0.1667	1.8333	0.1667
0.5	0.1667	1.5	0.3333
0.1667	1.3333	4.5	3.8333
1.3333	0.1667	4.8333	3
12	0.1667	0.5	8.5
10.667	7.5	4.8333	
0.8333	1.6667	2.3333	
0.1667	0.3333	0.5	
2.5	2.3333	4	
0.5	1.3333	1.5	
1	0.8333	2.1667	
0.1667	1.3333	1.3333	

Table C. Lengths of the dry blocks of rain rate averages converted to units of hours over a 4×4 km^2 region of TOGA-COARE in sequence by column.

TABLE D			
0.1667	1.5	0.1667	0.1667
0.1667	0.8333	1.8333	1
0.3333	1.3333	3.5	0.6667
0.1667	5.5	2	1.3333
0.5	0.6667	0.1667	0.5
6.3333	0.1667	0.1667	0.1667
1.6667	0.1667	0.3333	2.3333
0.1667	7.8333	1.1667	0.1667
0.1667	0.8333	0.1667	1.5
0.5	0.1667	0.3333	1.6667
0.1667	0.3333	0.1667	0.1667
1.8333	0.8333	0.5	0.5
1	0.1667	0.1667	0.3333
1	0.1667	2.1667	0.3333
0.1667	0.1667	2.5	0.8333
1.1667	0.1667	0.3333	1.5
0.5	0.1667	3.1667	1.3333
0.1667	2.1667	2.8333	0.5
1.3333	1.3333	3	0.6667
2.8333	0.6667	0.3333	0.3333
0.5	0.5	0.3333	0.5
0.1667	0.5	0.1667	0.6667
0.5	0.5	0.6667	0.1667
0.1667	0.3333	1.1667	0.8333
0.1667	0.3333	0.1667	0.5
1.3333	0.1667	0.1667	0.3333
0.5	0.6667	0.1667	1
2.3333	0.6667	0.1667	0.3333
3.5	0.1667	0.1667	0.5
0.3333	0.1667	0.8333	0.5
0.1667	0.1667	0.1667	0.1667
0.1667	0.5	0.3333	0.5
0.1667	0.3333	0.3333	1.1667
0.1667	0.1667	0.1667	0.1667
0.1667	0.3333	2	0.3333
0.6667	3.1667	0.1667	0.1667
1	0.3333	0.8333	0.1667
0.1667	0.3333	3.5	0.5
0.3333	0.1667	0.3333	0.8333
2.3333	0.5	0.6667	

Table D. Lengths of the wet blocks of rain rate averages converted to units of hours over a 4×4 km^2 region of TOGA-COARE in sequence by column.

TABLE E			
0.3333	0.3333	0.5	0.3333
1.1667	0.3333	0.1667	0.6667
0.6667	0.6667	1.5	7.1667
0.1667	0.3333	0.1667	0.6667
0.6667	0.3333	0.1667	0.8333
4.5	3.3333	0.1667	9
0.1667	0.6667	0.1667	0.3333
0.1667	0.5	0.3333	1.3333
0.1667	0.3333	5.6667	0.1667
0.8333	1	1	4.8333
1.8333	5.6667	0.5	2.1667
0.6667	0.1667	1.3333	2.5
0.1667	3.8333	7.1667	1.5
0.5	10.8333	0.6667	0.1667
0.1667	1.3333	0.1667	1.1667
2.6667	0.1667	0.3333	2
0.1667	1	0.1667	0.1667
0.3333	0.5	0.3333	0.8333
1.1667	8	2.6667	0.8333
0.3333	0.1667	0.1667	8.8333
0.5	0.8333	1.8333	0.5
2.8333	0.3333	3.6667	0.1667
0.1667	1.1667	7.5	0.3333
0.6667	0.1667	9	0.5
3	0.1667	1.6667	0.1667
2.8333	7.5	1.5	3.8333
1.8333	1.5	4.5	3
0.1667	0.3333	4.5	8.5
0.3333	2	0.5	0.5
0.1667	1.3333	4.8333	
1.3333	0.1667	1.5	
12	1.3333	0.5	
10	0.1667	0.5	
0.5	0.1667	3.1667	
0.6667	2	0.5	
0.1667	5	1.5	
2.3333	0.1667	2.1667	
0.8333	3.1667	1.1667	
0.1667	0.3333	1.1667	
0.1667	0.3333	1.5	

Table E. Lengths of the dry blocks of rain rate averages converted to units of hours over a 6×6 km^2 region of TOGA-COARE in sequence by column.

TABLE F							
0.1667		6.3333		0.3333		1.3333	
0.3333		0.1667		0.3333		0.6667	
0.5		0.1667		0.5		0.1667	
0.1667		7.8333		0.1667		4.6667	
0.1667		0.8333		2.3333		0.3333	
0.5		0.1667		2.5		1.6667	
0.1667		1.6667		0.3333		0.3333	
6.3333		0.3333		3.1667		0.5	
1.8333		0.5		2.8333		0.3333	
0.3333		0.6667		3		0.3333	
1		0.1667		0.1667		1	
0.1667		0.1667		0.1667		1.5	
3.1667		2.1667		0.3333		1.3333	
0.1667		1.3333		0.3333		1.8333	
1.1667		0.6667		0.1667		0.8333	
1.5		0.5		0.1667		0.8333	
0.8333		1.6667		0.6667		0.1667	
1.3333		0.3333		1.1667		1.1667	
3		0.1667		0.1667		0.1667	
1.5		0.6667		0.1667		1	
0.1667		0.6667		0.5		0.8333	
0.1667		0.1667		0.1667		1	
0.3333		0.5		1		0.8333	
1.3333		1.5		0.3333		0.6667	
0.5		0.1667		0.1667		1	
2.5		0.3333		0.1667		0.1667	
3.6667		3.1667		0.3333		0.5	
0.3333		0.3333		0.3333		1.6667	
0.1667		0.5		0.3333		0.8333	
0.1667		0.1667		2		0.1667	
0.1667		0.8333		0.3333		0.1667	
0.1667		0.3333		1		0.5	
0.1667		2.3333		3.5		0.8333	
0.3333		3.6667		0.3333		0.3333	
0.6667		2		0.1667			
1.1667		0.1667		0.8333			
0.1667		0.1667		0.1667			
3.3333		1.8333		0.1667			
1.6667		0.1667		1.1667			
2.6667		0.1667		0.6667			

Table F. Lengths of the wet blocks of rain rate averages converted to units of hours over a 6×6 km^2 region of TOGA-COARE in sequence by column.

TABLE G			
0.1667	5.6667	0.6667	1.0000
1.1667	0.1667	1.0000	0.5000
0.5000	1.8333	0.1667	0.8333
0.6667	1.6667	3.1667	8.8333
4.5000	10.8333	0.8333	0.3333
0.8333	1.0000	2.1667	0.1667
1.8333	0.1667	3.0000	0.5000
0.6667	1.0000	0.3333	0.1667
0.1667	0.1667	1.0000	3.8333
0.1667	3.6667	3.1667	3.0000
2.3333	4.0000	4.5000	8.5000
0.1667	0.1667	1.6667	0.1667
0.3333	0.8333	1.5000	
0.5000	0.3333	1.5000	
0.3333	0.8333	2.6667	
0.5000	0.1667	4.5000	
0.3333	7.5000	0.3333	
2.3333	1.1667	0.1667	
0.6667	0.1667	4.3333	
3.0000	0.1667	1.5000	
2.8333	2.0000	0.3333	
1.8333	1.3333	0.1667	
0.3333	0.1667	2.1667	
0.1667	1.3333	0.8333	
0.1667	0.1667	0.1667	
0.1667	1.8333	1.0000	
0.5000	1.5000	0.8333	
0.3333	5.0000	1.0000	
0.1667	0.1667	1.0000	
7.1667	0.1667	1.1667	
3.3333	2.5000	1.3333	
1.3333	0.1667	0.3333	
1.5000	0.3333	0.1667	
6.8333	0.3333	0.3333	
0.5000	0.1667	0.6667	
0.6667	1.5000	6.3333	
2.3333	0.1667	0.5000	
0.6667	0.1667	0.5000	
0.1667	0.1667	9.0000	
0.1667	0.3333	0.1667	
0.3333	5.5000	0.3333	
0.6667	0.8333	0.6667	
0.3333	0.5000	0.1667	
0.3333	1.3333	4.8333	
1.5000	7.1667	2.1667	
1.6667	0.6667	2.5000	
0.6667	0.3333	1.3333	
0.5000	0.1667	0.1667	
0.3333	0.1667	1.0000	
0.8333	2.6667	0.1667	

Table G. Lengths of the dry blocks of rain rate averages converted to units of hours over a 8×8 km^2 region of TOGA-COARE in sequence by column.

TABLE H				
0.1667	2.6667	0.1667	0.3333	0.8333
0.3333	6.8333	1.8333	0.3333	0.6667
1.0000	0.1667	0.1667	1.0000	1.6667
0.1667	7.8333	0.1667	3.6667	0.5000
9.3333	0.8333	0.1667	0.1667	1.6667
0.3333	0.1667	0.6667	0.5000	0.8333
1.0000	0.1667	0.5000	0.3333	0.1667
0.1667	1.6667	0.5000	1.0000	0.1667
0.1667	0.3333	0.3333	0.3333	0.5000
0.1667	0.5000	2.3333	0.1667	1.0000
2.8333	0.6667	3.0000	0.3333	0.6667
0.8333	0.1667	3.1667	1.6667	
0.1667	0.3333	2.8333	0.8333	
4.8333	2.1667	3.0000	0.1667	
1.5000	1.3333	0.3333	1.6667	
0.1667	0.1667	0.1667	0.6667	
0.5000	0.8333	0.5000	0.1667	
0.3333	0.5000	0.5000	4.8333	
1.3333	0.1667	0.1667	0.3333	
0.5000	2.1667	0.1667	0.1667	
6.3333	0.3333	0.6667	1.6667	
0.3333	0.8333	1.5000	0.1667	
0.3333	0.1667	0.1667	0.3333	
0.1667	0.8333	0.6667	0.6667	
0.1667	0.1667	0.1667	0.6667	
0.3333	0.5000	1.5000	0.3333	
0.3333	1.5000	0.1667	1.1667	
0.3333	0.1667	0.1667	0.1667	
0.1667	4.0000	0.1667	1.6667	
0.1667	0.3333	0.5000	1.3333	
0.1667	0.1667	0.1667	1.8333	
0.1667	0.5000	0.1667	0.8333	
0.1667	0.3333	0.1667	1.0000	
0.1667	0.8333	0.8333	0.1667	
0.3333	0.3333	0.1667	1.3333	
0.6667	2.3333	0.1667	0.1667	
1.5000	5.8333	0.3333	0.3333	
3.3333	0.1667	0.3333	2.6667	
1.8333	0.3333	2.0000	1.1667	

Table H. Lengths of the wet blocks of rain rate averages converted to units of hours over a 8×8 km^2 region of TOGA-COARE in sequence by column.

TABLE I									
0.5		0.5		0.8333		0.1667		0.6667
0.1667		2.1667		0.1667		0.6667		1.1667
1.1667		0.1667		1.8333		0.1667		1.1667
0.5		0.1667		5		0.1667		0.3333
0.6667		0.1667		0.3333		2.5		0.1667
3.1667		0.1667		0.5		0.6667		0.1667
1.1667		0.6667		0.3333		1		0.6667
0.6667		0.3333		0.1667		0.1667		6.3333
1.8333		0.3333		2		1.8333		0.5
0.6667		0.6667		1.1667		0.1667		0.3333
0.1667		0.5		1.1667		0.1667		8.8333
0.1667		1.5		0.1667		0.3333		0.1667
2.3333		0.1667		1.8333		0.8333		0.5
0.1667		0.3333		1		2.1667		0.1667
0.1667		0.3333		0.3333		3		3.8333
0.1667		0.1667		4.5		0.1667		0.1667
0.3333		0.6667		0.3333		1		2
0.3333		4.3333		0.1667		3.1667		2.3333
0.3333		1.1667		0.1667		4.5		1.3333
2.1667		0.1667		2.5		1.5		1
0.6667		1.8333		0.1667		1.1667		0.1667
3		1.6667		0.1667		1.5		0.8333
2.8333		6		0.1667		2.6667		0.5
1.8333		0.1667		1.5		4.1667		0.5
0.3333		0.6667		0.1667		0.1667		8.5
0.1667		1.3333		0.1667		4.3333		0.1667
0.5		2		12.3333		1.5		0.5
0.3333		0.8333		0.1667		0.3333		0.1667
0.1667		0.1667		0.3333		0.1667		3.8333
7.1667		0.8333		5.1667		2.1667		3
3.1667		0.1667		0.1667		0.6667		8.5
1.3333		3.6667		0.8333		1		0.1667
1.3333		4		0.5		0.3333		
6.8333		0.1667		1.1667		0.1667		
0.5		0.6667		6.8333		1		

Table I. Lengths of the dry blocks of rain rate averages converted to units of hours over a 10×10 km^2 region of TOGA-COARE in sequence by column.

TABLE J										
0.1667		3.5		0.1667		0.3333		0.3333		
0.3333		2.1667		4		0.1667		1.6667		
1		2.6667		0.1667		0.6667		1		
0.1667		7		0.1667		1.5		0.1667		
0.1667		0.1667		0.3333		1.1667		5		
9.5		7.8333		0.1667		0.1667		0.3333		
0.3333		0.8333		1		1.6667		0.3333		
1		0.1667		0.3333		0.1667		1.6667		
0.1667		0.1667		0.8333		0.1667		0.1667		
0.1667		0.5		3		0.1667		0.3333		
0.1667		1.6667		6		0.1667		0.6667		
2.8333		0.1667		0.1667		0.1667		0.8333		
1		0.5		0.3333		0.1667		1.8333		
0.5		0.8333		0.1667		0.6667		0.3333		
5		0.6667		0.1667		0.1667		1.8333		
1.5		0.5		1.8333		0.1667		1.3333		
0.1667		0.3333		0.1667		0.1667		0.6667		
0.6667		0.1667		0.1667		1		2		
0.3333		2.1667		0.1667		0.1667		1.1667		
1.3333		1.3333		0.1667		0.1667		1		
0.5		0.1667		0.6667		0.3333		1.6667		
0.3333		0.8333		0.5		0.5		0.1667		
0.8333		0.1667		0.6667		2.3333		0.3333		
0.5		0.1667		3		0.3333		2.8333		
0.3333		0.1667		6.3333		0.5		1.3333		
0.3333		0.1667		2.8333		1.1667		1.3333		
0.3333		0.6667		3.1667		4.1667		2.6667		
0.1667		0.1667		0.1667		0.5		0.5		
0.3333		2.1667		0.1667		0.3333		1.8333		
0.3333		0.5		0.3333		1		0.8333		
0.1667		0.8333		0.1667		0.3333		0.1667		
0.1667		0.1667		0.1667		0.1667		0.1667		
0.1667		0.8333		0.5		2.3333		0.5		
0.5		0.1667		0.5		0.8333		1		
0.8333		2.5		0.1667		0.1667		1		

Table J. Lengths of the wet blocks of rain rate averages converted to units of hours over a 10×10 km^2 region of TOGA-COARE in sequence by column.

APPENDIX

The following table contains the estimated quantities obtained from the data of Dry and Wet durations (the original data exist in the Tables A-J). These quantities are very useful, because they are used for the parameter estimation of Lognormal, Inverse Gaussian, and Gamma distributions (MLE or MME).

AREA KM^2	EPOCH DURAT-IONS	NUM. OF OBSERVA-TIONS	$\sum X_i$	$\sum X_i^2$	$\sum \log X_i$	$\sum\left(\frac{1}{X_i}-\frac{1}{\bar{X}}\right)$	$\sum(\log X_i-\hat{\mu})^2$	GEOME-TRIC MEAN
10 ×10	DRY	172	244.5	1004.53	-65.63	325.52	249.027	0.6828
	WET	175	182.83	587.36	-110.19	354.19	212.35	0.533
8 ×8	DRY	162	247.1672	1034.748	-47.0295	281.3991	232.3799	0.7480
	WET	167	168.834	517.4139	-105.3523	323.3656	191.9568	0.5321
6×6	DRY	149	264.6673	1370.555	-32.8135	262.96	236.5749	0.8023
	WET	154	152.1674	386.694	-90.8547	277.186	169.5448	0.5544
4×4	DRY	153	275.33	1459	-37.14	288.8	256.6	0.7845
	WET	159	133.17	313.14	-117.94	302.51	158.81	0.4763
2×2	DRY	138	297.67	2212.28	-14.841	246.44	245.36	0.8980
	WET	144	109.83	229.42	-121.03	296.56	143.2947	0.4315